Models for Estimation of Service Life of Concrete Barriers in Low-Level Radioactive Waste Disposal

Prepared by J. C. Walton, L. E. Plansky, R. W. Smith

Idaho National Engineering Laboratory
EG&G Idaho, Inc.

Models for Estimation of Service Life of Concrete Barriers in Low-Level Radioactive Waste Disposal

Prepared by
J. C. Walton, L. E. Plansky, R. W. Smith

Idaho National Engineering Laboratory
Managed by the U.S. Department of Energy

EG&G Idaho, Inc.
P.O. Box 1625
Idaho Falls, ID 83415

Abstract

Concrete barriers will be used as intimate parts of systems for isolation of low-level radioactive wastes subsequent to disposal. This work reviews mathematical models for estimating the degradation rate of concrete in typical service environments. The models considered cover sulfate attack, reinforcement corrosion, calcium hydroxide leaching, carbonation, freeze/thaw, and cracking. Additionally, fluid flow, mass transport, and geochemical properties of concrete are briefly reviewed. Example calculations included illustrate the types of predictions expected of the models.

Summary

Concrete barriers are likely to be incorporated into low-level radioactive waste disposal facilities as structural components and barriers to fluid flow and mass transport of radionuclides. Analysis of the role of the concrete barriers in low-level waste isolation requires that performance assessment models be applied to concrete degradation. Because the history of modern concrete is short (~100 years) relative to the required prediction of service life, the task is difficult and subject to uncertainty.

This report consists of a critical review of mathematical models that predict concrete material properties over long time periods. Models obtained from the literature are explained in enough detail to illustrate derivation and basic assumptions. Additional example calculations are included to illustrate application of the models and to indicate the types of predictions that can be expected   m the models.

Degradation processes important to waste isolation include sulfate attack, reinforcement corrosion, leaching, carbonation, freeze thaw, and stress cracking. A brief review of mass transport and fluid flow through concrete is provided. The transport material provides consistent nomenclature for the calculations in the models. Examples of the range of water chemistry expected in subsurface environments in the United States and an overview of concrete pore water chemistry and its potential influence on radionuclide mobility are provided. Basic knowledge of concrete chemistry is necessary for applying the degradation models. The background sections are followed by individual chapters covering the mathematical models for each class of degradation. A future report will evaluate the implications of degradation and general design for performance of the concrete vault.

Acknowledgements

Contents

Figures

Tables

Acronyms

ACI   American Concrete Institute

ASTM   American Society for Testing
        and Materials

BFS   Blast furnace slag

CSH   Calcium silicate hydrate

DME   Dyanmic modulus of elasticity

LLW   Low-level waste

OPC   Ordinary Portland Cement

PCA   Portland Cement Association

SRPC   Sulfate Resistant Portland Cement

WCR   Water-to-cement ratio

MODELS FOR ESTIMATION OF SERVICE LIFE
OF CONCRETE BARRIERS
IN LOW-LEVEL RADIOACTIVE WASTE DISPOSAL

INTRODUCTION

Concrete barriers are likely to be incorporated into low-level radioactive waste disposal facilities as structural components and barriers to fluid flow and mass transport of radionuclides. Analysis of the role of the concrete barriers in low-level waste (LLW) isolation requires that performance assessment models be applied to concrete degradation. Because the history of modern concrete is short (~100 years) relative to the required prediction of service life, the task is difficult. The task is made even more difficult by the great importance of quality assurance and workmanship. These aspects are of crucial importance to durability but difficult to quantify and include in models. Another large problem is that the majority of models tend to be empirical in nature. Because the determinations of service life are of necessity longer than the empirical database, the empirical models are almost always applied outside the bounds of the initial data. Blind extrapolation of empirical data is difficult to defend technically, but is frequently the only option to no prediction at all.

This report consists of a critical review of mathematical models that predict concrete material properties over long time periods. Models obtained from the literature are explained in enough detail to illustrate derivation and basic assumptions. Additional example calculations are included to illustrate application of the models and to indicate the types of predictions that can be expected from the models.

Degradation processes important to waste isolation are listed in Table 1. Models have been found that attempt to cover sulfate attack, reinforcement corrosion, leaching, carbonation, freeze/thaw, and stress cracking. A brief review of mass transport and fluid flow through concrete is provided. This transport material provides consistent nomenclature for the calculations in the models. Examples

of the range of water chemistry expected in subsurface environments in the United States and an overview of concrete pore water chemistry and its potential influence on radionuclide mobility are provided. Basic knowledge of concrete chemistry is necessary for application of the degradation models.

The background sections are followed by individual chapters covering the mathematical models for each class of degradation. Example calculations and graphs are included in several sections and illustrate the types and range of predictions to be expected from some of the models. These calculations are nominally organized along the lines of vaults located in different portions of the United States; however, associations between soil chemistry and region are approximate. A future report will evaluate the implications of degradation and general design for performance of the concrete vault.

Table 1. Categories of concrete degradation phenomena

Sulfate Attack	Carbonation
Reinforcement Corrosion (Chloride Attack)	Skrinkage Cracking Thermal Cracking Miscellaneous Cracking
Stress Cracking	Alkali-Aggregate Reaction
Leaching of Concrete Constituents	Freeze/Thaw Damage
Acid Attack	Oxidation and Biodegradation of Coatings and Sealants

CHEMICAL ENVIRONMENT

Chemicals Important to Concrete Durability

The loss of durability of concrete is caused either by the external environment or internal causes. The external causes can be physical, chemical, or mechanical. Internal causes of degradation are the alkali-aggregate reaction, volume changes due to differences in thermal properties of aggregate and cement paste, and most importantly, the permeability of the concrete. Permeability of the concrete is important in limiting mass transport of corrosive agents (e.g., sulfate, chloride) into the concrete and leaching of cement components [e.g., $Ca(OH)_2$] from the concrete.

The near field environment, as considered herein, constitutes the soil and soil moisture conditions directly surrounding and in contact with the concrete structure as well as the wastes contained inside the concrete vault. The near field environment is considered from the perspective of the concrete.

A number of chemicals are important to concrete degradation. These have been identified by the American Concrete Institute (ACI) and summarized by the Portland Cement Association (PCA) (PCA, 1986). In general, most acids attack either the cement itself or the steel reinforcement. Salts and alkalies known to cause degradation include: salts containing sulfate, bisulfite, cyanide, dichromate, fluoride, hexametaphosphate, nitrate, or chloride ions; sodium perborate, sodium perchlorate, potassium persulfate, sodium phosphate, thiosulfate; ammonium superphosphate; and borax. Petroleum oils generally do not lead to degradation; some coal tar distillates such as creosote may cause slow disintegration. Most solvents and alcohols do not lead to degradation. Exceptions are carbon disulfide, glycerin, and ethylene glycol, which lead to slow degradation. Many vegetable and animal oils lead to concrete degradation.

In typical disposal situations, the ions in the soil environment of greatest concern are sulfate, chloride, carbon dioxide, and magnesium. Because these ions are ubiquitous, model development has focused on their effects. In general, mathematical models are not available to evaluate the concrete degradation caused by the multiple other chemicals that could be present in the waste. Current models have been developed almost entirely from the perspective of external attack on the concrete from the soil side.

Soil Moisture Chemistry Importance and Dependencies

Soil moisture levels and the chemistry of soil moisture are important to the siting of waste repositories. Soil moisture can be an important transport medium for radionuclides. It can affect the performance of a disposal site through chemical degradation phenomena, such as sulfate or chloride attack. Soil pH and Eh also affect the sorption and precipitation mechanisms that can control radionuclide mobility.

The soil moisture chemistry of a potential disposal site is dependent upon environmental factors. These factors include soil source material, drainage, proximity to oceans, and climate, especially the balance between precipitation and evapotranspiration. In humid environments, soils become leached of soluble salts, leading to low ion concentrations in soil moisture. As precipitation rates fall relative to evaporation, soluble salts begin to accumulate in the soil, leading in extreme cases to saline soils. Although climate is very important, source rock type, drainage, and location are also of great importance. Locations near oceans typically experience higher chloride levels.

Examples of Different Soil Moisture Chemistries

Examples of soil moisture chemistry at different locations in the United States (Table 2) were obtained from several sources. These data represent chemical analyses of stream flow, springs, soil moisture collected from suction lysimeters, and precipitation. Stream flow represents a composite of precipitation, runoff, and infiltrated water. In humid regions, this is a reasonable estimate of typical soil water composition. In arid, mountainous regions, stream flow may be dominated by snowmelt and runoff that will differ greatly from soil moisture in chemical composition.

The data indicate arid regions may have increased concentrations of chloride and sulfate, making them much more aggressive towards concrete. The aggressive composition of the soil moisture in arid regions is balanced against lower infiltration rates and amounts of moisture that contact the concrete.

Processes such as leaching are relatively more important in humid situations whereas arid environments may produce specific attack on the concrete barrier components (e.g., sulfate attack, chloride attack).

Table 2. Water chemistry characteristic of several locations in the United States.

Constituent (mg/l)	Humid Northern [Hubbard Brook] (Likens et al., 1977)	Midwestern [Mississippi River] (Hem, 1970)	Arid Western [INEL] (Laney et al., 1988)	Precipitation [Hubbard Brook] (Likens et al., 1977)	World River Water (Hem, 1970)
Sulfate	6.3	56	1430	2.9	11
Chloride	0.55	30	3150	0.47	7.8
Magnesium	0.38	12	372	0.04	4.1
Bicarbonate	0.92	132	125	0.0006	58
pH	4.92	7.5	--	4.14	
Dissolved Oxygen		10	--		
Silica		6.7	81		13
Calcium	1.65	42	488	0.1	15
Potassium	0.23	2.9	36	0.07	2.3
Sodium	0.87	25	1652	0.12	6.3
Dissolved Solids		256	7315		90

Constituent (Horne, 1978) (ppm)	Big Spring, Huntsville, AL Limestone	Jumping Springs, Eddy County, NM Gypsum	Cooks Springs, Colusa, CA Serpentine	Well, San Miguel County, NM Shale	Salt Banks, Chrysotile, AR	Well, Owyhee County, ID
Sulfate	4.0	1570	6.0	303	882	30
Chloride	3.5	24	390	80	16,000	10
Magnesium	4.2	43	614	31	286	1.4
Bicarbonate	146	143	4090	445	1,490	111
pH	7.0				7.1	9.2
Silica	8.4	29	80	13	45	99
Calcium	46	636	26	30	496	2.4
Dissolved Solids	139	2,410	3760	973	28,400	348

FLOW AND TRANSPORT THROUGH CONCRETE

Fluid flow and mass transport through a concrete vault are two of the most important factors influencing concrete degradation rates and the ability of the concrete to assist with isolation of the waste. Over time as a concrete vault ages, the properties of the concrete and its ability to assist with isolation of the waste will change. Portions of the concrete will crumble and become more permeable. Eventually cracks will penetrate the concrete slabs, leading to preferential pathways through the barrier. This section reviews some of the aspects of flow and transport through concrete that are relevant to understanding the mathematical models for concrete degradation. The performance implications of the degradation phenomena will be treated in more detail in a future document.

Fluid Flow Through Matrix

The rate of water percolation through a waste isolation system is one of the most important measures of performance. Initial matrix permeability of cement paste is influenced strongly by water-to-cement ratio (WCR) with its influence upon capillary porosity (Powers, 1958 and 1960). Evaluation of fluid flow is complicated by location of the low-level waste (LLW) facilities in the unsaturated zone.

Flow through the unsaturated zone can be described using the Richard's equation (Hillel, 1971).

$$\frac{\partial \theta}{\partial t} = \frac{\partial}{\partial x}\left(K(\psi)\frac{\partial \psi}{\partial x} \right) + \frac{\partial}{\partial z}\left(K(\psi)\left(\frac{\partial \psi}{\partial z} - 1 \right) \right) \qquad (1)$$

where

ψ = pressure head (cm)

θ = volume content

K = conductivity (cm/s).

Compared to other components of the vault system, the typical pore sizes in concrete are very small. Soils can be dried to near the residual saturation at suctions of a few bars (Wosten and van Genuchten, 1988), while removal of water from cement or concrete requires tensions of hundreds to thousands of bars (Daian, 1988). For example, concrete can maintain 85% saturation at tensions of 9 bars (Daian, 1988). The small pore sizes are especially characteristic of low WCR concretes used for concrete barriers. In subsurface environments, the small pores in the concrete successively remove water from the surrounding materials leading to saturation of the concrete matrix. The concrete matrix remains near saturation even when the surrounding soils are quite dry.

The hydraulic conductivity of gel pores is approximately 7×10^{-16} m/s (Powers, 1958). The permeability of the cement paste is a function of capillary porosity. Capillary porosity in turn is dependent upon the WCR and degree of hydration. Typical cement paste has a permeability of 20 to 100 times the minimum (Powers, 1958). In general, the hydraulic conductivity of concrete with a low WCR should be less than 10^{-12} m/s.

Fluid Flow Through Cracks

Approach. Even in relatively minor amounts, cracking can lead to orders of magnitude increases in saturated hydraulic conductivity of concrete. If the concrete is one of the more significant barriers to flow through the system, the increase in hydraulic conductivity can lead to proportional increases in water percolation through the system.

Location of the LLW facilities in the unsaturated zone greatly complicates the role of cracks in influencing performance of concrete barriers. In unsaturated environments, water remains in a state of tension created by capillary action (absorption) and adsorption. Because cracks are large relative to the pore size of the matrix, they have a limited ability to hold water in tension. In other words, under unsaturated conditions cracks will drain quickly. The drained cracks not only no longer contribute to flow but may also serve as barriers to flow (Wang and Narasimhan, 1985). Depending upon the degree of saturation, cracks may range from orders of magnitude increases in flow rate to significant decreases in flow relative to an uncracked specimen. The ability of cracks to hold water (and thereby contribute to flow) as a function of pressure head is illustrated in Figure 1.
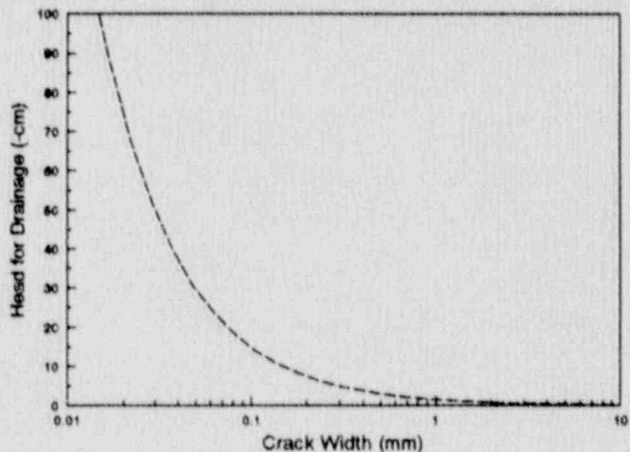
Figure 1. Suction head for crack drainage under partially saturated conditions.

Saturated System. The permeability of intact concrete with low water to cement ratio is very low. For this reason, cracks, particularly microcracks, are thought to actually control concrete permeability in service environments. Microcracks are caused by a variety of phenomena including response of concrete and reinforcement bars to physical loading, drying shrinkage, and expansion/contraction from temperature changes.

If an infinitely long, parallel sided crack through the concrete is assumed, the flow though a crack is

$$K = \frac{\rho g b^2}{12\mu} \tag{2}$$

where

  k = hydraulic conductivity (cm/s)

  ρ = density of water (g/cm³)

  g = acceleration of gravity (980 cm/s²)

  b = fracture aperture (cm)

  μ = viscosity of water (~0.01 g/cm s).

Studies of flow through cracks in concrete slabs have shown that actual flow is typically 1/3 to 2/3 of the theoretical value (Loadsman et al., 1988). A value of 1/2 is applied giving (Figure 2)

$$K = \frac{\rho g b^2}{24\mu}. \tag{3}$$
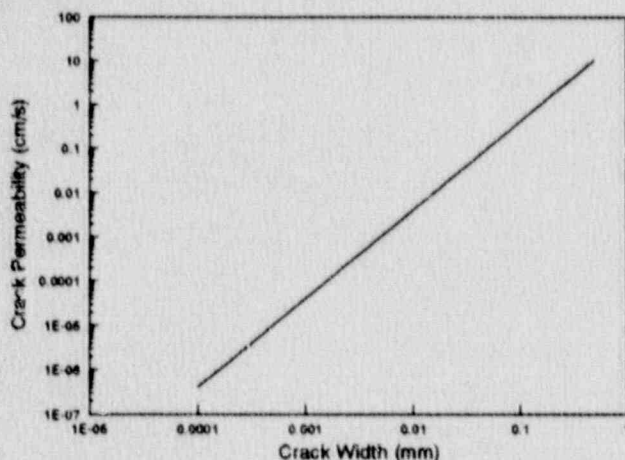
Figure 2. Individual crack hydraulic conductivity for concrete as a function of crack width.

More generally desirable is the contribution of a series of cracks to overall or average permeability of a slab. If s is the crack spacing (cm/crack) for evenly spaced cracks of constant aperture, then the proportional area of cracks is $A_c = b/s$, and the bulk permeability of the cracked slab is

$$K = \frac{\rho g b^3}{24\mu s} + K_{mat}. \tag{4}$$

Usually the matrix permeability (K_{mat}) is much less than the crack permeability and can be ignored.

Partially Saturated Systems. The above analysis assumes that all cracks are saturated. For concrete vaults located in the unsaturated zone, this is not always the case. The pressure head for drainage of a crack of width b is

$$h = \frac{-2\gamma \cos(\alpha)}{b\rho} \tag{5}$$

where

  γ = surface tension of water (72.7 dyne/cm)

  α = cement water contact angle (assumed = 0)

  h = pressure head (cm).

Thus, the crack width giving permeability increase at any given pressure head is the greatest width that will not be drained or

$$b_{max flow} = \frac{-2\gamma \cos(\alpha)}{h\rho g} = \frac{-0.148[cm^2]}{h}. \tag{6}$$

Mass Transport Through Cement and Concrete Matrix

Overview. The primary modes of radionuclide transport in an intact concrete are advection/dispersion and diffusion through the matrix. The transport of fluids and chemicals through the concrete is also the single most important factor in controlling concrete degradation. This is evidenced by the importance of WCR - which determines the final concrete porosity and permeability to durability (Powers, 1960).

Other modes of transport that may become significant are nonaqueous liquid phase movement (e.g., organic liquids in the waste) and gaseous transport. An example of gaseous transport scenario is when tritiated water reacts with steel containers and/or reinforcement bars leading to the formation of hydrogen gas

$$3Fe(c) + 4H_2O \Rightarrow Fe_3O_4(c) + 4H_2(g). \tag{7}$$
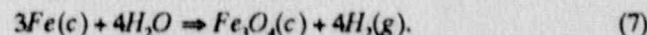
The rate of escape of the hydrogen gas is then important to system performance. Gaseous transport can also be significant in influencing the oxidation-reduction status of the interior of the vault. Oxidation-reduction conditions in turn are important in influencing metal corrosion rates and radionuclide mobility (solubility/sorption).

Diffusion Transport Parameters. In relatively impermeable materials such as intact concrete, the rate of water flow is very low. In low flow situations, diffusional transport according to Fick's laws of diffusion will dominate mass transport. Diffusion of dissolved species can occur in either the gaseous or liquid phase. Because of the small pore sizes concrete matrix present in belowground vaults remains near saturation with water even when the surrounding soil

5

materials are relatively dry. Thus, it is anticipated that most diffusional transport in subsurface concrete barriers will be through the liquid phase, irrespective of whether the vault is located above or below the water table.

The general transport equation for aqueous transport assuming linear partitioning between liquid and solid is (Codell and Duguid, 1983)

$$\theta \frac{\partial C}{\partial t} = \frac{1}{R_d} \vec{\nabla} \cdot (\theta D_E \vec{\nabla} C - \vec{V} C) - C \frac{\partial \theta}{\partial t} - \lambda \theta C. \tag{8}$$

The retardation factor is given by

$$R_d = 1 + \frac{\rho_b}{\theta} K_d \tag{9}$$

where

R_d = retardation factor

C = concentration (g/cm^3)

λ = decay constant (s^{-1})

K_d = distribution coefficient (ml/g)

D_E = effective dispersivity/diffusivity (cm^2/s)

V = Darcy velocity

θ = volumetric water content $(cm^3 \text{ water}/cm^3 \text{ total})$

ϕ = porosity $(cm^3 \text{ voids}/cm^3 \text{ total})$.

Diffusional flux of contaminants dissolved in liquids is estimated from Fick's First Law

$$F = -\theta \tau D \vec{\nabla} C = -\theta D_E \vec{\nabla} C = -D_i \vec{\nabla} C \tag{10}$$

where

D = tracer diffusion coefficient in water (cm^2/s)

D_E = effective diffusion coefficient (used in transport equation) (cm^2/s)

D_i = intrinsic diffusion coefficient (measured in steady state flux experiments) (cm^2/s)

τ = tortuosity factor.

If linear reversible sorption is assumed, Equation 2 reduces to

$$\theta \frac{\partial C}{\partial t} = \frac{1}{R_d} \vec{\nabla} \cdot (\theta \tau D \vec{\nabla} C) - C \frac{\partial \theta}{\partial t} - \lambda \theta C \tag{11}$$

where

C = concentration in liquid (g/cm^3)

λ = decay constant (s^{-1})

D = dispersivity (cm^2/s)

ρ_b = bulk density (g/cm^3).

Discussion. There are several potential problems caused by a lack of standardization of nomenclature in the diffusion literature. Because the nomenclature used in the literature for the different types of diffusion coefficients is highly variable and inconsistent, we have attempted to apply a consistent nomenclature in this report as defined in Equation (10). Several different approaches found in the literature are discussed below.

The tortuosity factor can be expressed as

$$\tau = \frac{\delta}{\tau_o^2} \tag{12}$$

where

δ = constrictivity

τ_o = tortuosity.

Since tortuosity and constrictivity corrections generally appear as a single lumped factor in experimental work, simplicity is maintained by using a single parameter (τ).

Atkinson and Nickerson (1988) define a capacity factor (α) and relate it to the distribution coefficient in the following manner:

$$\alpha = \phi + (1 - \phi)\gamma, \tag{13}$$

which is equivalent to

$$\alpha = \phi + (1 - \phi)\rho_s K_d = \phi + \rho_b K_d = \phi R_d. \tag{14}$$

The total concentration of contaminant in the concrete, assuming full liquid saturation, is

$$C_t = \phi C_i + (1 - \phi)C_s = C_i \alpha. \tag{15}$$

Substituting into the diffusion Equation (11) the following is obtained

$$\frac{\partial C_t}{\partial t} = \vec{\nabla} \cdot \frac{\phi \tau D}{\alpha} \vec{\nabla} C_t - \lambda C_t = \vec{\nabla} \cdot D_a \vec{\nabla} C_t - \lambda C_t \tag{16}$$

where

D_a = $(D\tau\phi)/\alpha$

γ = volumetric distribution coefficient (dimensionless)

ρ_s = density of the solid (g/cm^3)

α = capacity factor (dimensionless).

Using the Atkinson nomenclature the diffusional flux of contaminant can be expressed as

$$F = D_a \vec{\nabla} C_t. \tag{17}$$

In Crank (1975), the diffusion equation with linear sorption is expressed as

$$\frac{\phi \partial C_i}{\partial t} = \frac{1}{1 + R} \vec{\nabla} \cdot \phi D \vec{\nabla} C. \tag{18}$$

6

If (1+R) is replaced with R_f and D with D_E in the above equation, then we have the form used in Equation (8).

It is very important to carefully define and understand the meaning of all the terms when applying the transport equation. Consistency must be maintained between the conventions used in the experimental determinations of diffusion coefficients and in the use of diffusion coeffic.. n in performance assessments.

Experimental Diffusion Results. In the absence of radioactive decay, steady-state flux is independent of sorption. Sorption delays the time for attainment of steady-state, but does not impact steady-state flux. If radioactive decay is significant, then sorption will lower the steady-state flux.

Most diffusion coefficients obtained in the literature result from measurement of steady-state flux. The reported (intrinsic) diffusion coefficients lump the tracer diffusion coefficient in water, the porosity, and tortuosity into one parameter. Atkinson *et al.* (1984) report laboratory and literature results for intrinsic diffusion coefficients as a function of the WCR. These results are fit to an equation of the form

$$\log D_i = 6wcr - 9.84$$

or

$$D_i = \phi \tau D = 1.45 \cdot 10^{-10} \exp(13.8wcr) \tag{19}$$

where

    D_i = intrinsic diffusion coefficient (cm^2/s)

    wcr = water-to-cement ratio (by mass).

The results are illustrated in Figure 3. In the lower range of WCRs (0.2 to 0.44), characteristic of well-designed concrete engineered barriers, the intrinsic diffusion coefficient ranges from 10^{-9} to 10^{-7} cm^2/s.

The porosity of concrete is dependent upon WCR, curing, and the porosity of the aggregate. Powers (1958) reports that the densest possible completely hydrated cement paste has a porosity of about 28%. This occurs at a WCR of around 0.35 - 0.40. Porosity lower than 28% in cement paste can only be generated by the presence of unhydrated cement.

Figure 4 illustrates the porosity data from Alford and Rahman (1981). The data has been fit to a curve of the form
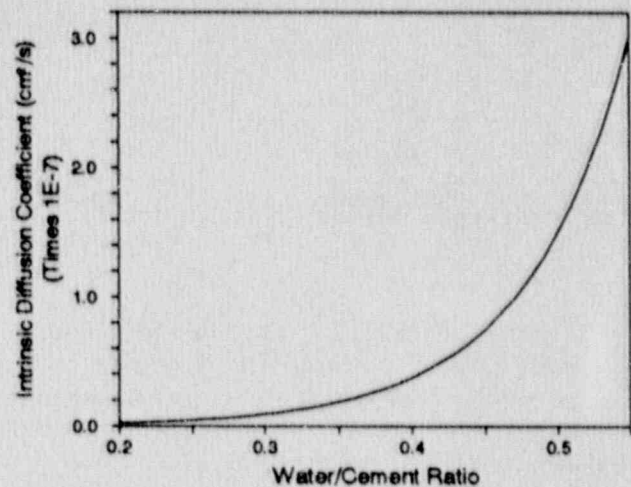
Figure 3. Intrinsic diffusion coefficient in cement paste as a function of WCR.

$$\phi = 0.61 + 0.23 \ln(wcr). \tag{20}$$

In the interest of generality, most reasearch on cement properties is performed with cement past in the absence of aggregate. When examining the literature on concrete and when preparing performance assessment calculations, one must be careful to distinguish between the two. Generally about 60-75% by volume of concrete is aggregate.
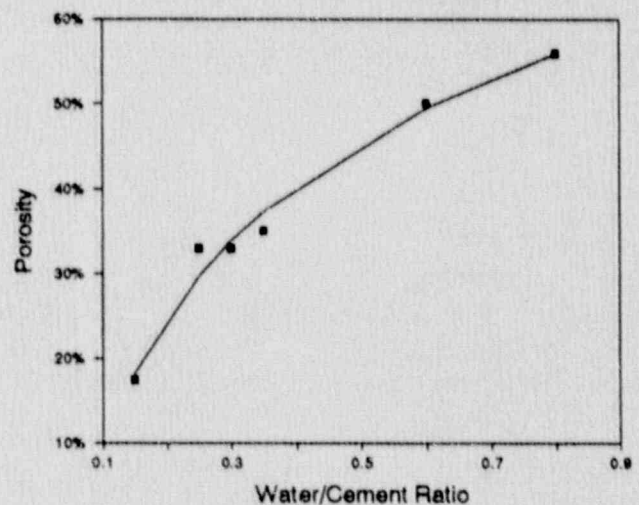
Figure 4. Relation between WCR and porosity.

The decomposition of measured diffusivity into individual components of porosity, tortuosity, and diffusion coefficient in water becomes important when transient diffusional processes are considered. Transient diffusional fronts move more rapidly when the tortuosity factor is high. Thus, a low tortuosity factor is favorable for waste isolation. Combination of the empirical relationships for porosity of cement and effective diffusivity gives an estimate of tortuosity factor as a function of WCR.

7

$$\tau = \frac{D_i}{D\phi} \approx \frac{1.45 \cdot 10^{-10} \exp(13.8wc)}{(0.61 + 0.23 \ln(wc))10^{-5}}$$

$$\approx \frac{0.00145 \exp(13.8wcr)}{61 + 23 \ln(wcr)}. \tag{21}$$

The estimated tortuosity factor is illustrated in Figure 5. Note that the tortuosity factor declines with lower WCR. Thus, a lower WCR tends to slow transient diffusion rates and gives increased contaminant residence times as well as slow steady-state diffusional transport.
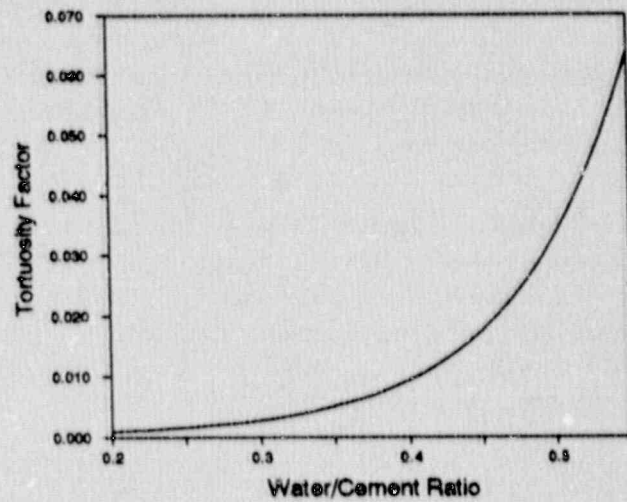
Figure 5. Estimated tortuosity factor for cement as a function of WCR.

8

SULFATE AND MAGNESIUM ATTACK

Sources of Sulfur and Magnesium

Sulfur. Sulfur generally occurs in the fully oxidized (S^{6+}) state when dissolved in water and is combined with oxygen as sulfate (SO_4^{2-}) ion. The reduced form of sulfur, sulfide (S^{2-}) occurs as the bisulfide ion (HS⁻) or undissociated H_2S in most soil water solutions, although the S^{2-} form may occur at the high pH of concrete. Conversion to and from the oxidized state is often associated with biochemical processes. Because of the slowness of sulfur oxidation or reduction reactions, nonequilibrium forms of sulfur can persist for long periods (Hem, 1970).

Sulfur is not a major constituent of the earth's crust, but is widely distributed in igneous and sedimentary rocks as metal sulfides. Weathering in contact with oxygenated water results in oxidation leading to the formation of sulfate ions. Sulfate occurs in certain igneous-rock minerals of the fieldspathoid group, but the most extensive occurrences are in evaporite deposits. Calcium sulfate as gypsum, $CaSO_4 \cdot 2H_2O$, or as anhydrite, which contains no water of crystallization, makes up a considerable part of many evaporite-rock sequences (Hem, 1970).

The second source of sulfate is from precipitation. At Hubbard Brook, New Hampshire, an extensively studied watershed, sulfate inputs exceed outputs indicating net accumulation of sulfate in the ecosystem (Likens et al., 1977).

Sulfate concentrations are increased in arid regions by evapotranspiration. This is especially important in regions where potential evapotranspiration exceeds precipitation.

Magnesium. The magnesium ion (Mg^{2+}) is normally the predominant form of magnesium in solution in natural water. The complex MgOH⁺ will be significant at pH > 10.0 (Hem, 1970).

In igneous rock, magnesium is typically a constituent of the ferromagnesian minerals. These include olivine, pyroxenes, amphiboles, and dark-colored micas. In metamorphic rocks, magnesian mineral species such as chlorite, montmorillonite, and serpentine occur. Sedimentary forms of magnesium include carbonates such as magnesite and hydromagnesite, brucite, and dolomite (Hem, 1970). Studies at Hubbard Brook indicate that output of magnesium consistently exceeds input from precipitation (Likens et al., 1977).

Magnesium may be added to sites in the form of dust suppressants such as $MgCl_2$ during or after construction.

Sulfate and Magnesium Attack

Sulfate reacts with tri-calcium aluminate (C_3A) to form calcium aluminum sulfates leading to expansion and disruption of the cement. A related problem is the reaction of magnesium with the cement to form Brucite [$Mg(OH)_2$].

Sulfate ions migrate into the concrete and react with the cement paste, forming gypsum and calcium sulphoaluminate. The products of the reaction have considerably greater volume than the compounds they replace, so that the reactions with the sulfates lead to expansion and disruption of the concrete. The reaction of sulfate with portlandite [$Ca(OH)_2$] to form gypsum, monosulphoaluminate, and ettringite can be written as

Gypsum:

$$Ca(OH)_2 + SO_4^{2-} + 2H_2O \Rightarrow$$

$$CaSO_4 \cdot 2H_2O + 2OH^- \qquad (1)$$

Monosulphoaluminate:

$$3CaO \cdot Al_2O_3 \cdot 6H_2O + CaSO_4 + 6H_2O \Rightarrow$$

$$3CaO \cdot Al_2O_3(CaSO_4) \cdot 12H_2O \qquad (2)$$

Ettringite:

$$3CaO \cdot Al_2O_3(CaSO_4) \cdot 12H_2O + 2CaSO_4 + 20H_2O \Rightarrow$$

$$3CaO \cdot Al_2O_3 \cdot 3(CaSO_4) \cdot 32H_2O. \qquad (3)$$
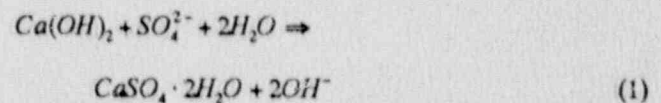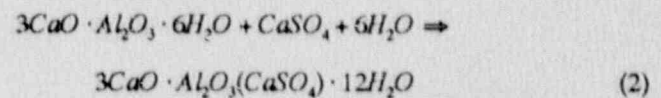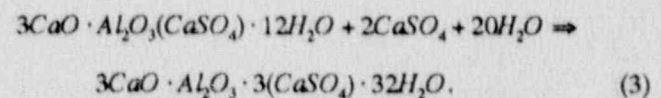
Studies on the behavior of concrete in sulfate soils (Stark, 1982) indicate that the WCR with its attendant impact upon porosity and permeability is the single most important factor affecting resistance to sulfate attack. C_3A content of the cement also significantly affects concrete durability in sulfate environments with a low C_3A content, leading to greater resistance to sulfate attack. Studies at the PCA (Klieger, 1980) indicated that the rate of sulfate attack in high sulfate soils was approximately proportional to C_3A content. Type V cement had a lifetime about 2-3 times as long as Type I cement. Performance had a greater dependence upon WCR than C_3A content. Moving from four bag to seven bag cement resulted in a 10-20 fold increase in lifetime.

An example of the reaction of cement paste with magnesium sulfate (Neville, 1981) is

$$3CaO \cdot 2SiO_2 + 3MgSO_4 \cdot 7H_2O \Rightarrow$$

$$3CaSO_4 \cdot 2H_2O + 3Mg(OH)_2 + 2SiO_2. \qquad (4)$$
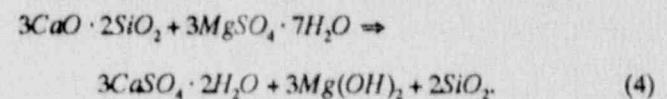
The low solubility of $Mg(OH)_2$ causes the reaction to proceed to completion, making the attack more severe. Further reaction between $Mg(OH)_2$ and silica gel is possible and may also cause deterioration.

Models of Sulfate and Magnesium Attack

Empirical (Atkinson and Hearne, 1984 and Atkinson *et al.*, 1985), shrinking core mechanistic models (Rasmuson *et al*, 1987), and more complete mechanistic models (Atkinson and Hearne, 1990) have been applied.

An empirically derived relation for sulfate attack was developed by Atkinson and Hearne (1984). Data collected in the Northwick Park study (Harrison and Teychenne, 1981) was used to develop the empirical model. The logic was as follows; The observed loss of cement at the corners of the blocks after 5 years in 0.19 M Na_2SO_4 solution was 42 mm. The cube experiments indicated that the depth of attack was linear with time. It was assumed that the rate of attack is proportional to sulfate concentration in the solution and tricalciumaluminate content of the cement. The depth of attack in $MgSO_4$ solution was approximately twice that in Na_2SO_4. Ordinary Portland Cement (OPC) with 8% C_3A had the greatest effects and was used as a reference material. These assumptions lead to the following equation

$$x = \frac{4.2}{5} \frac{C_s}{8} \frac{(Mg^{2+} + SO_4^{2-})}{0.19} t$$

$$= 0.55 C_s (Mg^{2+} + SO_4^{2-}) t \tag{5}$$

where

x = depth of deterioration (cm)

C_s = weight percent of C_3A in unhydrated cement

Mg^{2+}, SO_4^{2-} = concentration in bulk solution (mole/l)

t = time (yr).

A modified version of this empirical model is used in the Barrier code (Shuman *et al.*, 1989)

$$x = 1.86 \cdot 10^6 C_s (Mg^{2+} + SO_4^{2-}) D_i t \tag{6}$$

where

D_i = intrinsic diffusion coefficient in concrete (cm^2/s).

This relationship can be derived from Equation (1) by introducing the further assumptions that (a) the intrinsic diffusion coefficient in the experimental concrete blocks was 3×10^{-7} cm^2/s and (b) the rate of attack is proportional to the diffusion coefficient.

Empirical correlations have obvious limitations, expecially when applied outside the range of the basis data. Correlations are only valid over the range of the time/system parameters tested. Application outside of this range is highly questionable. The empirical correlation does not include the impacts of advective transport and/or the known importance of WCR or durability. Application of the empirical model is not clearly conservative. Notwithstanding these limitations, the simple empirical model is frequently the best option available for estimating resistance to sulfate attack (Figure 6).
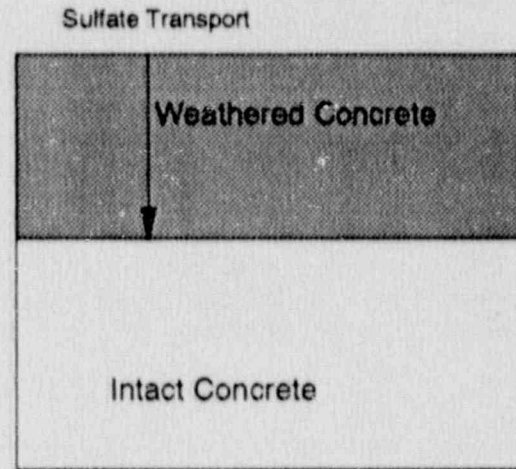
Sulfate Transport

Figure 6. Schematic of sulfate attack.

Shrinking Core Model. Shrinking core models have been used in chemical engineering where a moving boundary condition exists, but the rate of movement of the boundary is slow relative to transport rates. Because of the slow movement of the boundary, the mass transport processes can be considered to be always near steady state. This assumption is sometimes referred to as a series of stationary states.

In the case of sulfate attack, envision that sulfate ions migrate inward through weathered concrete to the boundary with intact, unweathered material. At the interface, the sulfate ions react with hydration products of tricalcium aluminate forming insoluble solids (e.g., ettringite). The mass transport equations are assumed to be always at steady state and are then used to estimate the rate of movement of the weathering zone into the concrete. The reactions are simplistically reduced to the format

$$SO_4^{2-} + X^{2+} \Rightarrow XSO_4^{2-}. \tag{7}$$

The flux of sulfate ions is given as

$$N = -D_i \frac{C_o}{x}. \tag{8}$$

The rate of movement of the weathering zone is then the rate of mass transport divided by the concentration of tricalcium aluminate in the solid

10

$$\frac{dx}{dt} = -\frac{N}{C_s} = \frac{D_i C_o}{C_s x} \qquad (9)$$

$$x = \left(\frac{2 D_i C_o}{C_s} t\right)^{\frac{1}{2}} \qquad (10)$$

where

C_s = concentration of tricalcium aluminate in the solid (moles/cm³)

C_o = concentration of sulfate in the bulk solution (moles/cm³)

x = distance (cm)

D_i = intrinsic diffusion coefficient (cm²/s)

N = molar flux [moles/(cm² s)]

t = time (s).

A more rigorous mathematical solution of the same problem, considering a full set of chemical reactions and rigorous solution of the mass transport equations, has also been applied to the problem (Rasmuson *et al.*, 1987) and gave similar results to the shrinking core model. The actual ratio of sulfate to C₃A is variable. For simplicity, a 1:1 ratio was assumed in the derivation.

Examination of the two formulae for sulfate attack (or taking derivatives) indicates that the impact of the C₃A content of the cement differs not only in magnitude but in sign. The empirical model predicts that sulfate attack rate will *increase* with increasing C₃A content while the shrinking core model predicts that the attack rate will *decrease* with increasing C₃A content of the cement. Thus, the shrinking core model is in direct conflict with experimental data and field experience with sulfate attack.

A second problem with the shrinking core or simple mass transport limitation to sulfate attack is that it predicts a square root of time dependence of the attack rate, whereas experimental data are consistent with a constant rate of attack.

Mechanistic Model. Atkinson and Hearne (1990) developed a mechanistic model for sulfate attack. The model considers sulfate attack as a three step process:

1. Sulfate ions penetrate the concrete, usually by diffusion

2. Sulfate ions react expansively with aluminium containing phases in the concrete

3. The resulting internal expansion causes stress, cracking, and exfoliation of concrete from the surface.

The process is dependent upon concrete composition, mass transport rates, and reaction rates. Reaction kinetics are estimated by

$$m = m_o \log_{10}\left(\frac{t_{spall} c_o}{t_r c_k}\right) \qquad m < m_c$$

$$m = m_c \qquad\qquad m > m_c. \qquad (11)$$

The concentration of reacted sulfate as ettringite (C_E) is given as

$$C_E = m \cdot \left(\frac{mass\ \ cement}{volume\ \ concrete}\right). \qquad (12)$$

The thickness of a layer that spalls off is given by

$$X_{spall} = \frac{2 \alpha \gamma (1 - v)}{E (B C_E)^2}. \qquad (13)$$

The time for the layer to spall is given by

$$t_{spall} = \frac{X_{spall}^2 C_E}{2 D_i c_o}. \qquad (14)$$

The degradation rate is given as

$$R = \frac{X_{spall}}{t_{spall}} = \frac{E B^2 c_o C_E D_i}{\alpha \gamma (1 - v)}. \qquad (15)$$

Depending upon the rate of diffusion relative to reaction rates, some iteration may be required to determine the proper value for C_E.

where

c_k = sulfate concentration in kinetic experiments (mol/m³)

c_o = sulfate concentration in bulk solution (mol/m³)

C_E = concentration of reacted sulfate as ettringite (mol/m³)

D_i = intrinsic diffusion coefficient (m²/s)

E = Young's modulus (20 GPa)

m = quantity of sulfate reacted with cement (mol/kg anhydrous cement)

m_c = value of m for complete reaction (mol/kg anhydrous cement) 1.24 for OPC and 1.07 for Sulfate Resistant Portland Cement (SRPC)

m_o = kinetic constant for m 0.32 for OPC and 0.16 for SRPC

R = concrete degradation rate (m/s)

t_r = characteristic time for reaction (s) 3577 for OPC and 1555 for SRPC

α = roughness factor for fracture path (assumed to be 1.0)

B = linear strain caused by one mole of sulfate reacted in 1 m³ (1.8×10^{-6} m³/mol)

γ = fracture surface energy of concrete (10 J/m⁻²)

v = Poisson's ratio (0.3).

In the example calculations given by Atkinson and Hearne (1990), the rate of attack for the sulfate resistant portland cement (SRPC) was approximately 30% lower than the attack rate for ordinary portland cement (OPC). This suggests that WCR (as reflected in the intrinsic diffusion coefficient) will be more important in controlling sulfate attack than the chemical composition of the cement. The importance of WCR in the mechanistic model is consistent with the observed importance of WCR in sulfate attack (Klieger, 1980).

Example Calculations

A few example calculations illustrate the types of concrete longevity predictions expected from the models for sulfate attack. Figures 7 through 9 represent predictions from the empirical model for sulfate attack. These graphs represent three different water chemistries that typify soil chemistry from around the United States. The different water chemistries are nominally labeled as northeast, midwest, and southwest locations. Actual performance calculations should utilize site specific chemical parameters; these calculations are only intended as illustrations.

Loss Degradation, cm
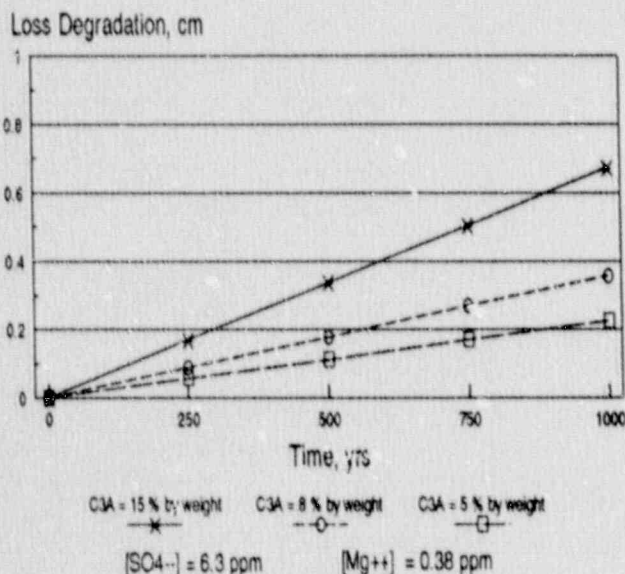
Figure 7. Estimates of sulfate attack in a low sulfate environment based upon empirical model.

The empirical model suggests that, from a standpoint of sulfate attack, concrete barriers will be much more effective in humid climates where sulfate levels are lower. However, the data upon that the empirical model is based do not include a situation where the water is forced to flow through the concrete (e.g, the situation with the roof of a concrete vault).

Results from the mechanistic model of Atkinson and Hearne (1990) are given in Figure 10. The graph is based upon the measurements for OPC and SRPC made in laboratory experiments. Because of the limited amount of data available for parameterization of the mechanistic model, it is difficult to directly compare empirical and mechanistic model predictions. The diffusion coefficient and the sulfate concentration are the most significant factors influencing resistance to sulfate attack, even more important than the type of concrete. High quality concrete with a low WCR will have a low diffusion coefficient leading to enhanced sulfate resistance.

Loss Degradation, cm
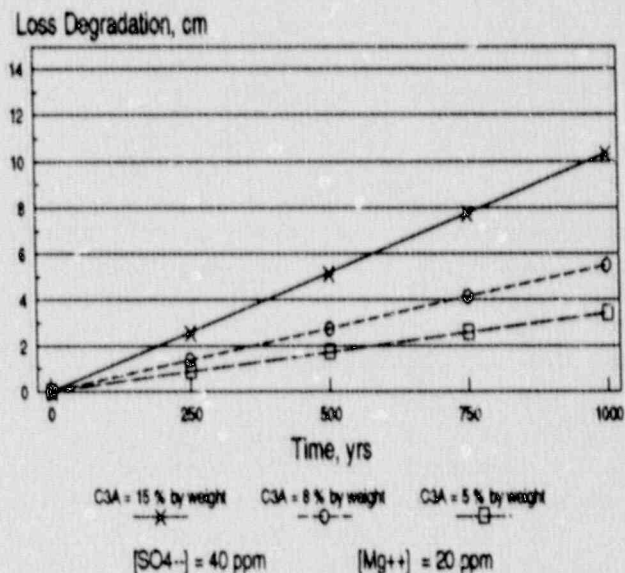
Figure 8. Estimates of sulfate attack rate in a midrange sulfate environment based upon empirical model.

Loss Degradation, cm
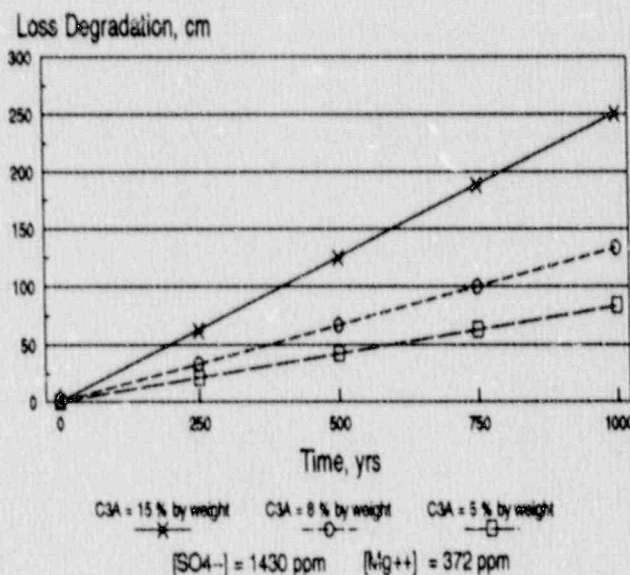
Figure 9. Estimates of sulfate attack rate in a high sulfate environment based upon empirical model.
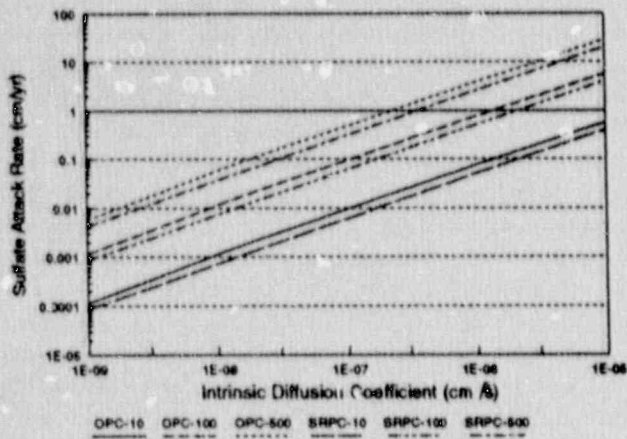
Figure 10. Estimates of sulfate attack rate based upon mechanistic model of sulfate attack. The lines represent calculations for OPC and SRPC at sulfate concentrations of 10, 100, and 500 ppm.

13

REINFORCEMENT CORROSION/CHLORIDE ATTACK

Reinforcement Corrosion

Steel reinforcement is used in concrete construction because the properties of the two materials are complementary. Steel has a very high tensile strength but less resistance to compressive stress. Concrete has low tensile strength but high compressive strength and is relatively inexpensive. These properties have led to widespread use of reinforced concrete beams and slabs.

The alkaline environment inside the concrete and isolation from external corrosive agents such as oxygen and chloride protect the steel reinforcement from corrosion by forming a protective oxide layer on the metal surface (Figure 11). As the concrete deteriorates and is subject to ingression of corrosive agents, the passive layer may undergo attack leading to active metal corrosion. Corrosion of the steel reinforcement, which occurs upon breakup of the passive layer, is important both from a structural standpoint and because corrosion can lead to concrete cracking.

Cracking of the concrete is caused because corrosion of steel results in corrosion products that significantly increase its molar volume. An example of the influence of different steel corrosion products upon volume taken from Walton and Sagar (1987) is given in Table 3. Expansion of the steel leads to spalling and disruption of the concrete. Reinforcement corrosion also lowers the strength of the steel, leading to potential structural instabilities.

The methodology for determining when reinforcement corrosion causes additional cracking is not straightforward. Loss of steel causes increased strain from physical loads on the structure. Additionally, the concrete can be expected to crack over the steel when the internal pressure generated by the corrosion products exceeds the tensile strength of the concrete.

Table 3. Volume changes resulting from steel corrosion.

Corrosion Products	Molar Volume (cm^3/mole)	Proportional Volume Increase
Iron (Fe)	7.09	-
Magnetite (Fe_3O_4)	44.5	2.1
Iron Sulfide (FeS)	17.6	2.5
Siderite ($FeCO_3$)	29.4	4.2

Breakup of the passive layer has historically been associated with the ingress of chloride ions into the concrete (ACI, 1985). Elevated levels of chloride lead to destruction of the passive layer because of specific attack or by serving as a supporting electrolyte in the solution. Chlorides are particularly important in concrete bridge decks where salt is added for deicing (Clear, 1976). The start of reinforcement corrosion is thought to be associated with a critical or threshold chloride level. Clear (1976) gives the chloride threshold as 0.02 mass percent of the cement paste. Subramanian and Wheat (1989) give the critical threshold level for chlorides in the pore solution as approximately 700 ppm. Recent work (Yonezawa et al., 1988) has evaluated the importance of good adhesion between steel and mortar as being of equal importance in influencing the start of corrosion in chloride solutions.

In the absence of elevated levels of chloride, reinforcement corrosion may begin when the alkalinity of the concrete is reduced, making the passive layer less stable. Processes such as carbonation and leaching lead to a gradual lowering of pH in concrete with eventual loss of passivity. Depassivation of the steel reinforcement can occur when the pH near the bars drops below 9 (Papadakis et al., 1989). Chloride attack predominates in marine or coastal environments or where deicing salts are applied to the concrete. Depassivation by lowering the concrete pH through carbonation or leaching may be more important in low chloride environments.

Chloride Attack   (passive layer breakup)
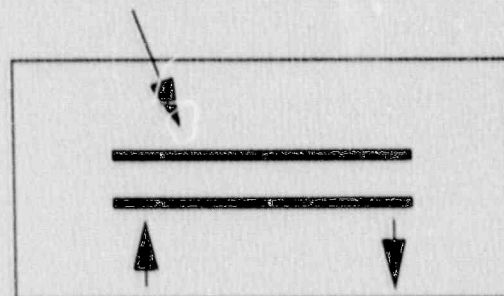
Oxygen Transport   Hydrogen Transport
(reactant)   (product)

Corrosion => Expansion => Cracking

Figure 11. Schematic of chloride attack on steel reinforcement.

Studies of steel corrosion in concrete slabs (Clear, 1976) clearly established that WCR and depth of cover over the reinforcement are the most important parameters affecting time until depassivation.

Sources of Chloride

Chloride is present as the chloride ion (Cl). In most soil environments, chloride acts as a conservative ion with relatively few chemical reactions.

Chloride is present in igneous rocks in lower concentrations than any of the other major constituents of natural water. Sedimentary rocks, particularly the evaporites, contain higher chloride levels (Hem, 1970).

Precipitation close to the oceans commonly contains from 1 mg/l to several tens of mg/l of chloride, but the concentrations observed generally decrease rapidly in a landward direction.

Studies at Hubbard Brook, New Hampshire (Likens *et al.*, 1977), indicate that chloride in this humid northern location is nearly at balance (i.e., input = output).

In arid regions, soil concentrations of chloride may be greatly elevated as a result of evaporation.

Chloride may be added to surfaces as a deicer and/or dust suppressant during construction or operation of the site.

Models of Chloride Attack

Chloride attack is modeled as a two stage process (a) time to breakup of the passive layer and initiation of corrosion and (b) corrosion rate subsequent to breakup of the passive layer.

Initiation. An empirical correlation for time to depassivation developed by Stratful and modified by Clear (1976) is

$$ t_c = \frac{129 x_c^{1.22}}{(WCR)[Cl]^{0.42}} \tag{1} $$

where

t_c = time to onset of corrosion (yr)

x_c = thickness of concrete over the rebar (in.)

WCR = water to cement ratio (by mass)

Cl = chloride ion concentration in groundwater (ppm).

The empirical equation clearly illustrates the impacts of cover over the steel and WCR on protection of the steel. The empirical model of Clear is used in the Barrier code (Shuman *et al.*, 1989).

A more complete mechanistic description of the problem is given by Bazant (1979a, 1979b). Bazant derives the governing equations for transport of chloride, oxygen, and water through the concrete. Subramanian and Wheat (1988) give the results of a one dimensional solution of Bazant's corrosion model.

An alternative for estimating the time to initiation of corrosion is to solve the mass transport equation for the arrival time of chloride. When the critical chloride level is reached at the depth of the reinforcement, breakup of the passive layer can be assumed to initiate.

The governing equation considering diffusion only transport can be given as

$$ \frac{C - C_{ini}}{C_{rw} - C_{ini}} = erf\left(\frac{X}{\left(\frac{4D_i t}{k_d}\right)^{\frac{1}{2}}} \right) \tag{2} $$

where

C = critical chloride concentration for initiation of corrosion

C_{ini} = initial chloride concentration in concrete pore water

C_{rw} = chloride concentration in the surrounding material

X = depth of cover over reinforcement.

The equation can be solved iteratively to obtain the time when the critical chloride threshold is reached at the level of the reinforcement.

Note that Equation (1), the empirical model, contains no provision for a chloride threshold - a serious but presumably conservative limitation. Equation (1) was derived from work related to bridge decks where salt is frequently applied for deicing. Application of the empirical equation to chloride concentrations typical of soils is clearly outside the range of the basis experimental data.

Simplified Corrosion Rate Calculation. The simplest method for estimating the corrosion rate subsequent to initiation of corrosion is a one dimensional diffusion calculation assuming limitation of the corrosion rate by oxygen diffusion.

The overall reaction is described by an equation such as

$$ Fe + \frac{3}{2}H_2O + \frac{3}{4}O_2 = Fe(OH)_3. \tag{3} $$
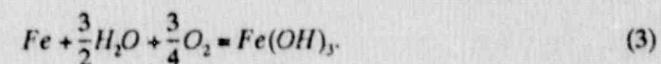
The flux of oxygen from the surface of the concrete to the level of the reinforcement is given by

$$ N_{O_2} = -D_i \frac{C_{rw}}{\Delta X}. \tag{4} $$

The resulting corrosion rate is then

15

$$R_{corrosion} = \frac{4}{3} N_{O_2} \frac{M_{Fe}}{\rho_{Fe}}$$

$$\approx 9.4 \left(\frac{cm^3}{mole} \right) D_i \frac{C_{gw}}{\Delta X}. \tag{5}$$

The amount of reinforcement per unit area of concrete is

$$\frac{\pi d^2}{4s}. \tag{6}$$

The percent of reinforcement remaining at any time is

$$\% \ remaining = 100 \left(1 - \frac{4 \cdot 9.4 \left(\frac{cm^3}{mole} \right) s D_i C_{gw} t}{\pi d^2 \Delta X} \right) \tag{7}$$

where

ΔX = depth of reinforcement below surface.

M_{Fe} = molecular weight of iron

ρ_{Fe} = density of reinforcement bars

C_{gw} = concentration of oxygen in surrounding groundwater

d = diameter of reinforcement

s = spacing between reinforcement bars.

In the Barrier code, a one dimensional steady state equation for the diffusion of oxygen is used with a zero concentration boundary condition at the metal surface. This type of calculation gives an upper bound to the contribution of oxygen reduction in saturated concrete. However elevated transport rates of gases in partially saturated concrete, advective transport, and/or the impact of the hydrogen evolution reaction are not considered.

Complex Models. Computer codes and models developed to evaluate container corrosion in radioactive waste repositories are also applicable to prediction of the corrosion rate of steel reinforcement. Harker et al., (1987) developed a one dimensional model for active corrosion of waste containers in concrete. Walton and Sagar (1987 and 1988) developed a general two dimensional model for active corrosion of steel in multiple layered geologic materials.

The models for active corrosion of steel assume that different combinations of mass transport and/or kinetics are rate limiting. In order to support oxidation of the steel through the reaction,

$$Fe(s) \leftrightarrow Fe^{2+} + 2e^-, \tag{8}$$
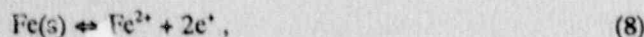
an oxidizing agent must be present. The oxidizing agents most appropriate for a concrete environment are oxygen gas and water. The kinetics of the oxygen reduction reaction can either be assumed to be transport limited or approximated with Butler-Volmer kinetics.

$$O_2(aq) + 2H_2O + 4e^- \Rightarrow 4OH^-(aq). \tag{9}$$
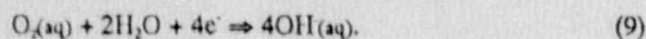
An example of an kinetic equation for the oxygen reduction reaction is (Turnbull, 1980)

$$i_{O_2} = kO_2 \exp\left(\frac{\alpha F E}{RT} \right) \tag{10}$$

$k = -4.9 \times 10 - 3 A/dm/mole$

$\alpha = -0.5$.

Because water is always available in a subsurface concrete environment and the overall reaction is favorable, the rate of the water reduction reaction must be estimated using kinetic expressions.

$$H_2O + e^- \leftrightarrow 0.5H_2(aq) + OH^-(aq) \tag{11}$$
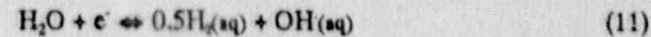
The Butler-Volmer equation written for this reaction is

$$E_{eq} = -2.303 \frac{RT}{F} \{ pH + 0.5 \log[H_2(g)] \} \tag{12}$$

$$k = 9.35 \times 10^{-10} \exp\left\{ \frac{\alpha_c F E_{eq}}{RT} \right\} \tag{13}$$

$$i_{H_2O} = k \left[-\exp\left\{ \frac{\alpha_c F}{RT} (E - E_{eq}) \right\} + \exp\left\{ \frac{\alpha_a F}{RT} (E - E_{eq}) \right\} \right] \tag{14}$$

$$\alpha_c = -0.5 \qquad \alpha_a = 0.5$$

where

E_{eq} = equilibrium potential from the Nernst Equation

E = corrosion potential versus SHE = $\phi_M - \phi_S$

α = transfer coefficient

i = current density (A/dm^2)

a, c = anodic, cathodic.

Anodic reaction kinetics are assumed to be active subsequent to the beginning of attack.

$$Fe(s) \leftrightarrow Fe^{2+} + 2e^+ \tag{15}$$
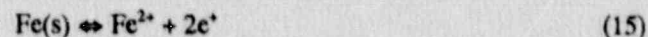
For active metal surfaces the anodic kinetics are described by the Butler-Volmer equation

$$E_{eq} = -0.44 + \frac{RT}{2F} \log(Fe^{2+}) \tag{16}$$

$$k = 1.99 \times 10^5 \exp\left\{ \frac{\alpha_a F E_{eq}}{RT} \right\} \tag{17}$$

$$i_{Fe} = k \left[-\exp\left\{ \frac{\alpha_c F}{RT} (E - E_{eq}) \right\} + \exp\left\{ \frac{\alpha_a F}{RT} (E - E_{eq}) \right\} \right] \tag{18}$$

$$\alpha_c = -1.0 \qquad \alpha_a = 1.0.$$

Mass Transport. The equation for transport of dissolved electrolytes in dilute solutions, subject to advection diffusion and electromigration, is (Newman, 1973)

$$\vec{J_i} = -nD_i \vec{\nabla} C_i - \frac{nz_i D_i F}{RT} C_i \vec{\nabla} \phi + VC \tag{19}$$

16

where

$\vec{J}$ = transport flux (moles/dm² s)

n = liquid porosity

D = diffusivity (dm²/s)

C = concentration (moles/dm³)

z = charge number

ϕ = electrostatic potential in solution (volt)

$\vec{\nabla}$ = vector gradient operator

V = Darcy Velocity (dm/s).

For uncharged species and/or when advection dominates the electromigration term becomes unimportant. Solution of the mass transport and chemical reaction equations (Walton and Sagar, 1987, 1988 and Harker *et al.*, 1987) suggests that oxygen levels quickly become depleted followed by buildup of hydrogen gas in the system. Corrosion rates then become limited by the diffusion rate of oxygen gas in the system and the kinetics of the hydrogen evolution reaction.

Example Calculations

The predictions of the simple models are illustrated in the following figures. Figures 12 through 15 give time to initiation of corrosion from Equation (1) as a function of WCR, chloride concentration, and depth of concrete cover over the reinforcement. The empirical equation contains no provision for a threshold chloride concentration and may be overly conservative. All of the graphs apply the empirical equation well outside the bounds of the data the equations were derived from with obvious implications for the quality of the predictions.

Figure 15 illustrates the calculated corrosion rate subsequent to initiation of corrosion assuming limitation by oxygen diffusion from Equation (7). Oxygen diffusion rates in actual systems become enhanced over time as processes such as calcium hydroxide leaching and sulfate attack lower the effective reinforcement cover thickness and increase mass transport rates. No attempt has been made to illustrate the coupled effects from multiple types of concrete attack in the example calculations.
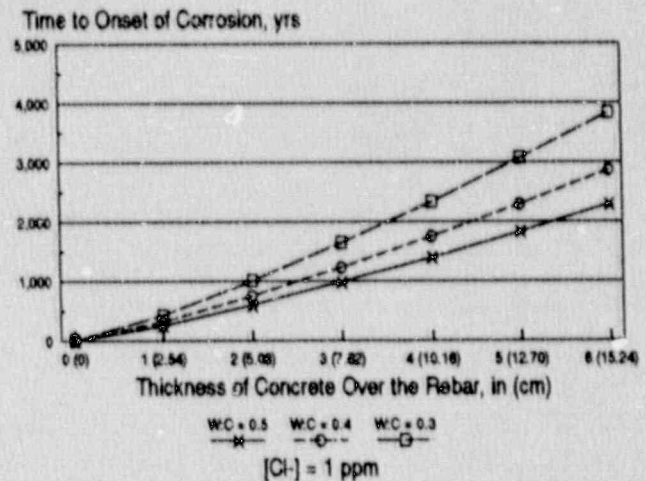
Figure 12. Time to initiation of reinforcement corrosion by empirical model as a function of WCR and depth of cover with soil chloride concentration of 1 ppm.
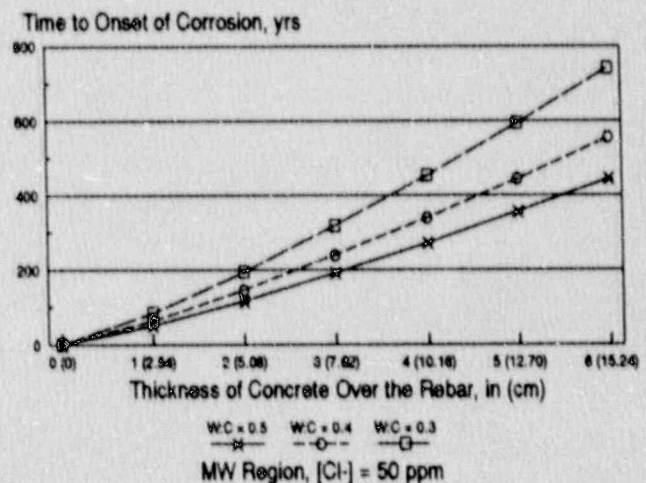
Figure 13. Time to initiation of reinforcement corrosion by empirical model with 50 ppm chloride in soil moisture.
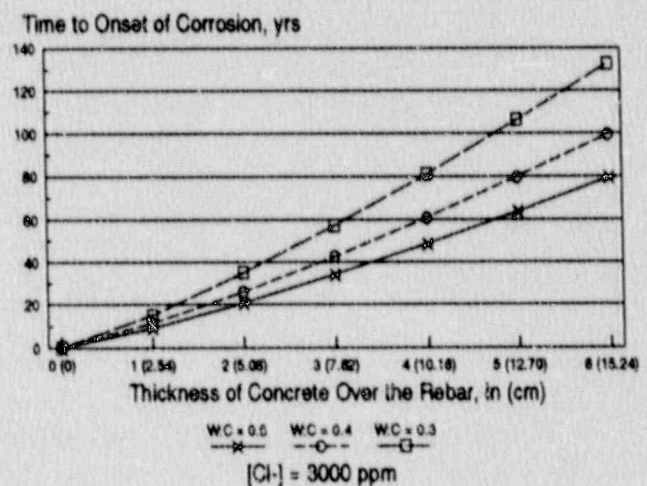
Figure 14. Time to initiation of reinforcement corrosion by empirical model with 3000 ppm chloride in soil moisture.

17

Percent Re-Bar Remaining

[Ca++] = 0.02 ppm, Water to Cement Ratio = 0.5
[O2]gw = 10 ppm, Di = 2E-8
1/2" Diam Rebar 2" below surface, 1' spacing
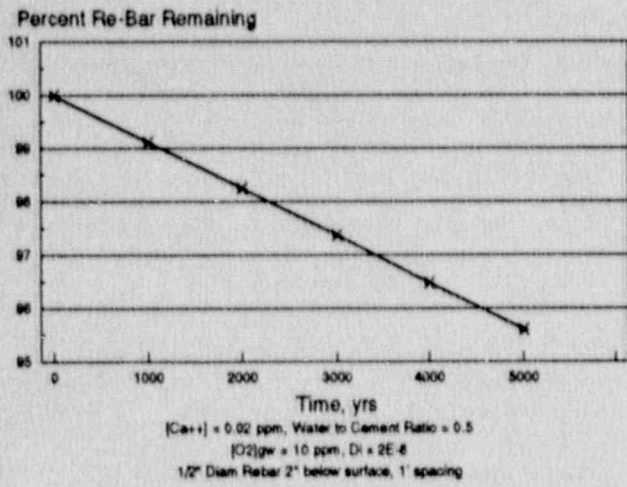
Figure 15. Example of oxygen limited corrosion rate subsequent to initiation of corrosion.

Cement components will be leached from concrete in environments that are in contact with water and have significant water percolation rates. The alkalis are initially affected followed by calcium hydroxide. The alkalinity of the concrete pore water decreases as the leaching process progresses.

Based upon modeling and experimental results, Atkinson (1985) and Atkinson et al. (1988) describe four stages of leaching. The time frames involved with each stage are dependent primarily upon water flow rates through the concrete. The four stages are

1. Initially, the pH is around 13 due to the presence of alkali metal oxides and hydroxides. The alkali metals are the first components to leach from the concrete.

2. After the alkali metals are leached, the pH is controlled at 12.5 by solid $Ca(OH)_2$.

3. Following loss of calcium hydroxide, the calcium silicate hydrate (CSH) gel phases begin to dissolve incongruently while the pH slowly moves down to 10.5. During this period, the calcium to silicon ratio drops to 0.85.

4. In the final phase, the pH is held at 10.5 by congruent dissolution of the CSH gel.

Leaching of calcium hydroxide tends to lower the strength of cement. The strength is lowered approximately 1.5% for every 1% of calcium lost (Lea, 1970). In advective environments, at least 66 m^3 of water is required to remove 33% of the calcium from 1 m^3 of typical concrete (Atkinson and Hearne, 1984).

Models of Leaching

Concrete Controlled Leaching. A shrinking core model has been applied by Atkinson and Hearne (1984) to evaluate leaching. The shrinking core model can be given by

$$Ca(OH)_2 \Rightarrow Ca^{2+} + 2OH^- \tag{1}$$

$$Flux = -D_i \frac{C_l - C_{gw}}{X} \tag{2}$$

$$\frac{dX}{dt} = \frac{D_i}{X} \frac{C_l - C_{gw}}{C_s} \tag{3}$$

$$X = \left(2D_i \frac{C_l - C_{gw}}{C_s} t \right)^{\frac{1}{2}} \tag{4}$$

where

C_l = concentration of Ca^{2+} in concrete pore waters liquid (moles/cm^3)

C_s = bulk concentration of Ca^{2+} in concrete solid (moles/cm^3)

D_i = intrinsic diffusion coefficient of Ca^{2+} in concrete (cm^2/s)

C_{gw} = concentration of Ca^{2+} in groundwater or soil moisture (moles/cm^3)

x = distance (cm)

N = molar flux [moles/(cm^2 s)]

t = time (s).

The shrinking core model assumes that removal of calcium from the exterior of the concrete is rapid relative to the movement through the concrete. Thus, the transport rate is controlled by diffusion in the concrete. Note that the formulation only includes diffusional mass transport. A more sophisticated model could include the influence of advection through and around the concrete. Because concrete is much less permeable than surrounding geologic materials, the dominant flow direction will rarely be normal to the concrete surface. Rather water tends to flow laterally around the concrete mass. This type of problem could be analyzed with two or three dimensional numerical flow and transport codes.

The intrinsic diffusion coefficient in the calculations applies to the leached or depleted portion of the concrete. Thus, it can be expected to be substantially higher than the D_i for intact concrete. The permeability of the concrete will also increase as leaching procedes, which leads to enhanced flow rates in the leached region (i.e., diffusion may no longer dominate transport).

Geology Controlled Leaching. An alternative formulation (Figure 16), also by Atkinson and Hearne (1984), assumes that diffusion into the surrounding geology is controlling. When diffusion is from a fixed concentration into a semi-infinite domain, then concentrations are described by an error function (Crank, 1975)

$$\frac{C - C_{gw}}{C_l - C_{gw}} = erf\left(\frac{X}{\left(\frac{4D_E t}{R_d} \right)^{\frac{1}{2}}} \right). \tag{5}$$

The instantaneous flux at X=0 is obtained by differentiation of the concentration profile

$$\left[\phi D_E \frac{\partial(C - C_{gw})}{\partial X} \right]_{X=0} = -\phi C_l - C_{gw} \left(\frac{D_E R_d}{\pi t} \right)^{\frac{1}{2}}. \tag{6}$$

The total amount of material leached (per unit area) during a given time period is obtained by integrating with respect to time

$$M_t = \phi C_i - C_{f\infty}\left(\frac{4R_d D_E t}{\pi}\right)^{\frac{1}{2}}. \tag{7}$$

The total amount of calcium hydroxide removed (per unit area) can be related to the inventory in the concrete as

$$M_t = X C_b \tag{8}$$

$$X = 2\phi\frac{C_i - C_{f\infty}}{C_b}\left(\frac{R_d D_E t}{\pi}\right)^{\frac{1}{2}} \tag{9}$$

where

C_i = concentration of calcium in the concrete pore water

C_b = concentration of calcium in the bulk concrete (solid + pores).

The assumption of surrounding geology limiting calcium hydroxide depletion is used in the Barrier Code (Shuman *et al.*, 1989). Note that the transport parameters (R_d, D_E, ϕ) in the geology controlled leaching model pertain to the surrounding geologic medium, not the concrete.
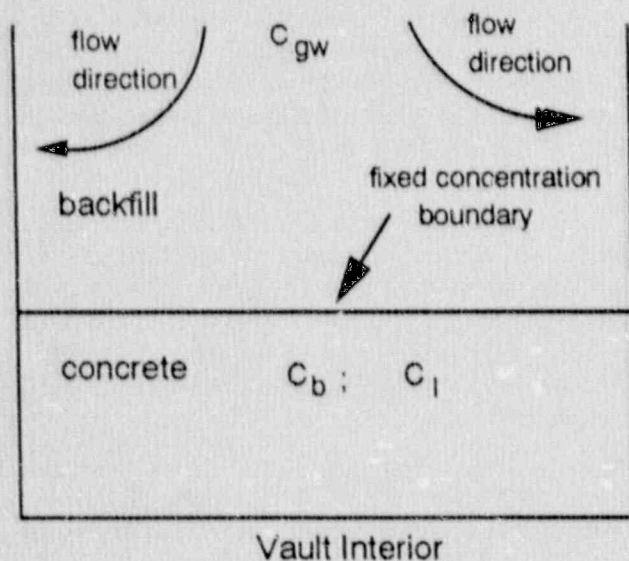
Figure 16. Schematic of calcium hydroxide leaching.

The impact of calcium hydroxide leaching has been estimated by assuming that the concrete loses half its strength when 33% of the calcium hydroxide has been depleted (Lea, 1970). Atkinson and Hearne (1984) simply assume the concrete fails when one third of the calcium in the layer is depleted. In the Barrier code (Shuman *et al.*, 1989), an exponential loss of strength is (apparently) assumed

$$Y = Y_e\left[1 - \left\{\left(\frac{X}{X_t}\right)\right\}^\alpha\right]. \tag{10}$$

Where Y is the yield strength of the concrete, Y_e is the initial yield strength, and X_t is the concrete thickness. Assuming that half the yield is lost at 33% depletion gives a value of 0.625 for α. The Barrier code documentation omits the normalization of X by X_t in the governing equation.

Alcorn *et al.* (1989) derive an expression for the change in hydraulic conductivity as a function of the change in porosity using data from different sources. The result is

$$\Delta K = K_0 \cdot 10^{(11.14^*\Delta\phi)} - K_0 \tag{11}$$

where

ΔK = the change in hydraulic conductivity of the concrete,

K_0 = initial hydraulic conductivity of the concrete

$\Delta\phi$ = change in porosity of the concrete.

The relationship is based on regressions of experimental data from various sources. The estimates from the equation are expected to be highly uncertain.

An analysis of combined geology and concrete controlled leaching along with fluid flow could be analyzed with numerical flow and transport codes if a more sophisticated approach was warranted.

Example Calculations

The predominant flow system for a concrete vault located in the vadose zone system is one of water moving around the concrete vault. This water could serve to remove calcium from the surface. The leaching process can be estimated using the shrinking core model (Atkinson and Hearne, 1984) for concrete controlled leaching. Figure 17 illustrates the predictions of the shrinking core model of leaching. Leaching is most rapid in locations with lower calcium concentrations.

Figure 18 illustrates the predictions for geology controlled leaching using the parameter assumptions listed on the figure.

Both sophisticated and simplistic models of leaching suggest that significant amounts of leaching require time frames in the thousands of years - quite long in the context of low-level radioactive waste disposal.

20
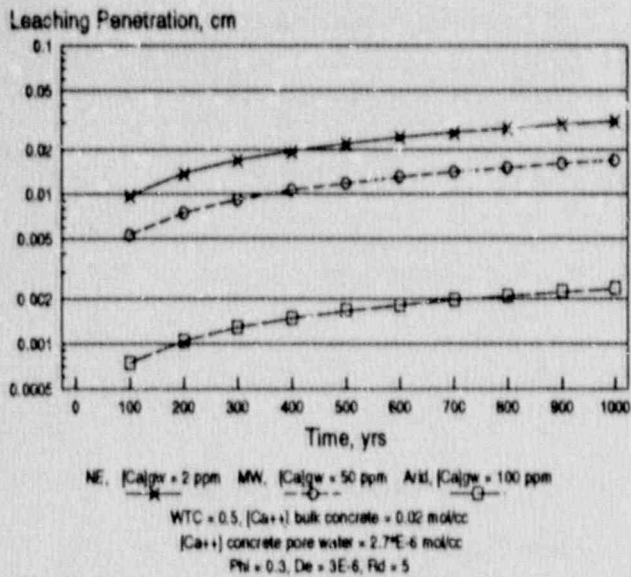
Figure 17. Calcium hydroxide leaching assuming concrete control in northeast, midwest, and arid environments.
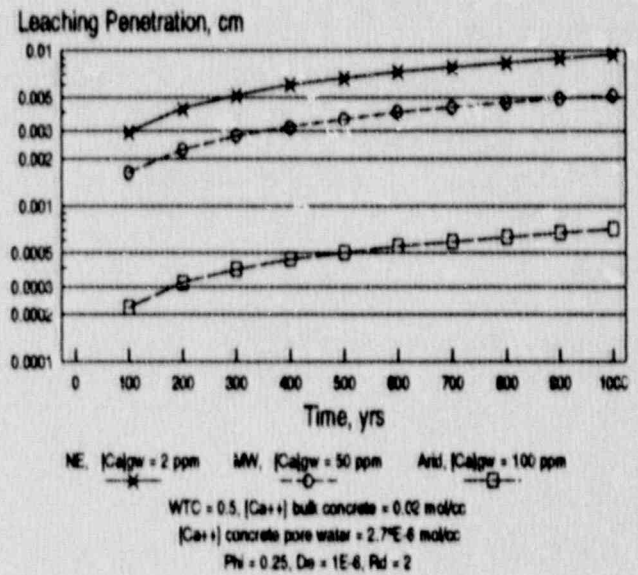
Figure 18. Calcium hydroxide leaching assuming geology control.

CARBONATION

Carbonation

Carbon dioxide reacts with cement components to form carbonates - a process referred to as carbonation. The reaction is represented by

$$Ca(OH)_2 + H_2O + CO_2 \Rightarrow CaCO_3 + 2H_2O. \qquad (1)$$
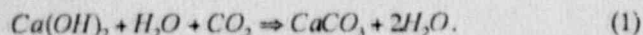
The depth of carbonation is roughly proportional to the square-root of time, doubling between 1 and 4 years, then doubling again between 4 and 10 years (Neville, 1981). The rate of carbonation depends upon the moisture content of the concrete and the relative humidity of the ambient medium. If diffusion in the concrete is too slow, an equilibrium is reached where the diffusion of CO_2 and carbonation are stopped or severely reduced. The type of cement ultimately affects the depth of carbonization.

Unlike other degradation processes, carbonation is not inconsistent with long-term durability of concrete. Carbonation does not cause general disruption or increased permeability of the concrete matrix. The formation of calcium carbonate may even slow migration of some radionuclides through solid solution reactions. Many concretes surviving from Roman times are fully carbonated. Carbonation is associated with two potentially negative changes in concrete material properties, shrinkage, and a drop in pH.

The total shrinkage from carbonation can be in the range of 0 to 0.1% (Verbeck, 1958). The shrinkage is thought to occur (Powers, 1962) as the minerals are removed from areas of compressive stress and redeposited in regions of lower stress. The compressive stress can occur as a result of capillary forces in a partially dried concrete. This can explain why carbonation under saturated conditions does not result in shrinkage since capillary forces are absent at saturation. The strength of concrete generally increases under carbonation, with the exception of high sulfate concretes. Carbonation of hydrated Portland-cement pastes also results in reduced permeability and increased hardness (Verbeck, 1958). The excess shrinkage may result in increased cracking and/or joint permeability. Carbonation forces the local pH toward neutral, going from over 12 to about 8, thereby removing some chemical barrier benefits of the concrete and providing a potentially corrosive environment for steel reinforcements if water, moisture, and oxygen can penetrate.

The rate of carbonation is dependent upon water saturation or relative humidity of the environment. As relative humidity increases from 0 to 100%, the rate of carbonation passes through a maximum. The maximum rate of carbonation occurs because water is required in the reaction of CO_2 and $Ca(OH)_2$ to form $CaCO_3$, but increasing water contents slow the diffusion rate of CO_2 through the concrete.

Sources of Carbon Dioxide

Carbon dioxide, in the presence of moisture, reacts with hydrated cement minerals in the form of carbonic acid. Carbon dioxide occurs as a minor constituent of air and a major component of carbonate rocks. Carbon dioxide is also generated from decomposition of organic materials in soils and/or waste.

Models of Carbonation Attack

Based upon Equation (1), a shrinking core model can be derived for carbonation. Carbonation can occur only as rapidly as dissolved carbonate can diffuse through the concrete. At the high pH relevant to concrete, Equation (1) actually occurs as

$$Ca(OH)_2 + CO_3^{2-} \Rightarrow CaCO_3 + 2OH^-. \qquad (2)$$
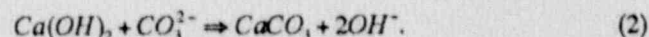
However, the transport of carbonate through the concrete can occur either as carbonate in the aqueous phase or carbon dioxide in the vapor phase. Since vapor phase diffusion is approximately four orders of magnitude more rapid than aqueous diffusion, one would expect rates of carbonation to increase as the saturation level of the concrete decreases - at least until the water required for the reaction becomes in short supply. Verbeck (1958) found that carbonation rates peak at 50% relative humidity, consistent with this observation.

A shrinking core model for carbonation can be formulated by evaluating the migration rate of CO_2 into the concrete in relation to the initial amount of calcium hydroxide. Although carbonation is most rapid at 50% relative humidity when significant amounts of water have been removed from the concrete, typical subsurface environments approach 100% relative humidity. Under these conditions, the concrete matrix remains water saturated because of the small pore sizes relative to surrounding soil materials. In most concrete vaults in the vadose zone, the transport of CO_2 is in the liquid phase, resulting in slow rates of carbonation. The following shrinking core derivation is valid for water saturated concrete:

$$Flux = -D_i \frac{C_{gw}}{X} \tag{3}$$

$$\frac{dX}{dt} = \frac{D_i}{X} \frac{C_{gw}}{C_s} \tag{4}$$

$$X = \left(2D_i \frac{C_{gw}}{C_s} t \right)^{\frac{1}{2}} \tag{5}$$

where

C_s = bulk concentration of $Ca(OH)_2$ in concrete solid $(moles/cm^3)$

D_i = intrinsic diffusion coefficient of Ca^{2+} in concrete (cm^2/s)

C_{gw} = concentration of total inorganic carbon in groundwater or soil moisture $(moles/cm^3)$

x = distance (cm)

N = molar flux $[moles/(cm^2\ s)]$

t = time (s).

Papadakis et al. (1989) have developed a rigorous mechanistic model for carbonation of concrete. The model considers mass transport, chemical reaction, and reaction kinetics. The model predicts that carbonation rates will peak as relative humidity is decreased from 100 to 50%. Below 50%, relative humidity reaction rates decline rapidly leading to slower rates of carbonation. In the range of 50 to 100% relative humidity, the model can be simplified to a shrinking core model similar to that given above. The derivation assumes partially saturated conditions (i.e., vapor phase diffusion of CO_2 dominates), thus the diffusion coefficient and concentration of CO_2 reflect vapor phase values.

Experimental values of the diffusion coefficient as a function of relative humidity are included in the paper (Papadakis et al., 1989).

Concrete degradation by carbonation is not (currently) considered in the Barrier code.

Example Calculations

The rate of carbonation by the shrinking core model is shown in Figure 19. The predicted rate of carbonation is slow for subsurface vaults because they are assumed to remain at full water saturation. Vaults that are located above the land surface or in highly desicated (i.e., desert) environments where relative humidity is significantly below 100% will experience more rapid rates of carbonation.
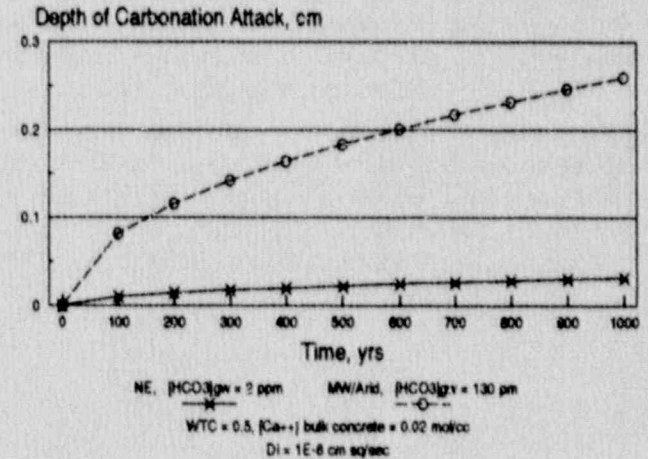
Figure 19. Rate of carbonation by shrinking core model in different geochemical environments.

ALKALI AGGREGATE REACTION

Aggregate is an additive to OPC that consists of particles of natural or artificial rock material of varying shapes ranging in size from tens of millimeters down to tenths of millimeters in cross section. Three quarters of the volume of concrete may be occupied by aggregate. Chemical reactions with the aggregate cause irreversible changes in concrete and play an important role in the physical, thermal, and chemical properties as well as in concrete durability and performance (Neville, 1981).

Three categories of deleterious substances may be found in aggregate (Neville, 1981): impurities that interfere with the cement hydration process, coatings that prevent the development of a good bond between the aggregate and the OPC paste, and weak or unsound aggregate particles.

A variety of processes may take place because of reactions between the components of the OPC and individual components or impurities of the aggregate, in particular, the reactions involving the alkali components of the cement paste (alkaline hydroxides derived from alkaline oxides in the cement) and the presence of active siliceous components in the aggregate (e.g., opal, chalcedony, or tridymite). An alkaline silica gel forms that alters the borders of the aggregate and leads to abnormal expansion, cracking, and loss of strength. This process is known as alkali aggregate reaction. Other degrading reactions of the aggregate include the oxidation of mineral oxides and sulfides or an alkali carbonate reaction - the reaction of carbonate in the aggregate with the alkali of the cement.

Alkali aggregate reaction can be reduced by the careful selection of aggregate and the elimination of the alkali components in the cement paste. It has also been found that the introduction of finely powdered reactive silica to the cement mix reduces or eliminates the reaction. This is due to the increased area of the reactive silica with less alkali per unit area being available (Neville, 1981). The alkali aggregate reaction is highly complex, and no mathematical models have been found to estimate its progression.

FREEZE/THAW

Concrete structures that are not buried below the local freezing depth will be subject to freeze/thaw cycles. Even structures built (or mounded) to depths below the freezing level will be subject to freeze/thaw processes during the operational phase of the facility. Upon freezing, water in the capillary pores of the concrete freezes and expands in volume by approximately 9%. Depending upon a variety of factors including number of freeze/thaw cycles, rate of freezing, concrete permeability, water saturation, water availability, aggregate, salt content, and amount of entrained air, degradation of the concrete can occur. Failure of the concrete generally takes the form of loss of strength and/or crumbling (Detwiler et al., 1989).

Two processes are considered to cause freeze/thaw damage (1) hydraulic pressure and (2) ice accretion (Detwiler et al., 1989; Clifton, 1990). Hydraulic pressure occurs when water in large pores expands upon freezing. The excess pressure can only be relieved when the excess water migrates to void spaces, such as the voids caused by air entrainment. Klieger (1980) suggests that osmotic forces may also be important during freezing. Salts in the solution are excluded from the ice crystals, leading to greater concentrations in the water moving away from the ice. The higher salt concentrations lead to counter osmotic forces that further increase the excess pressure. This proposed mechanism explains the negative impact that deicing chemicals have on freeze/thaw durability. The osmotic mechanism is a physical process consistent with experiments illustrating that widely different chemical compounds can have similar influences on freeze/thaw damage (Klieger, 1980). The hydraulic pressure mechanism is most important during rapid freeze/thaw cycles.

Ice accretion occurs when freezing causes a lowering of vapor pressure in the large pores. Water in the gel pores remains in a liquid state because of capillary attraction in the very small pores. Gel water freezes at a temperature below -78° C (i.e., gel water does not freeze in any expected service environments). The supercooled gel water then migrates to the large pores causing expansive forces around the large pores and compressive forces in the gel pores. The ice accretion mechanism is most important during extended periods of freezing (Detwiler et al., 1989).

Detwiler et al. (1989) list air entrainment, WCR, aggregate composition, and curing as the factors most important for making concrete that is resistant to freeze/thaw. Air entrainment works by providing open pores for relief of excess pressure. When air voids are properly spaced the local pressure will never exceed the tensile strength of the concrete resulting in a very resistant concrete.

Total freeze/thaw damage depends both upon the resistance of the concrete to freeze/thaw and the agressive properties of the service environment. Properties of the service environment that lead to damage are high water saturation of the concrete, large number of freeze/thaw cycles, and high salt content (Klieger, 1980). Typically a concrete has a critical water saturation level above which the material becomes very susceptible to damage.

Two testing methods for freeze/thaw resistance have been commonly used. These are contained in American Society for Testing and Materials (ASTM) Standard C 666-77. Both methods use rapid freezing first, but in one both freezing and thawing take place in water, while in the other freezing takes place in air and thawing in water. The former method is more severe than the latter (Neville, 1981). With these ASTM methods, freezing and thawing is done for 300 cycles or until the dynamic modulus of elasticity is reduced to 60% of its original value. A durability is computed from

$$durability\_factor = [(final\_number\_test\_cycles)$$

$$(\%\_of\_original\_modulus)]/300. \qquad (1)$$

There are no established criteria for the acceptance or rejection of concrete in terms of this durability factor. Its value is primarily for comparison of concretes. Usually, however, a factor smaller than 40 means the concrete is probably unsatisfactory with respect to freeze/thaw resistance or damage; 40 to 60 is the range for concrete with doubtful performance; and, above 60, the concrete is probably satisfactory (Neville, 1981).

Models of Freeze/Thaw Performance

Several models of freeze/thaw durability have been proposed. A review of several of the freeze/thaw models, as well as an introduction to the problem is given by Clifton (1990). The models range in complexity from empirical to a full solution of the fluid flow, temperature, and stress equations as proposed by Bazant et al. (1988). The discussion below covers the model used in the Barrier code (Shuman et al., 1989).

In the Barrier code, freeze/thaw durability is modeled by a fit of data that expresses the fractional decrease in dynamic modulus of elasticity (DME) of the concrete as a curve fit involving the % entrained air (AIR), water-to-cement ratio (WCR), and the number of freeze/thaw cycles. The variation of DME is taken to be linear when the number of freeze/thaw cycles is greater than 50; this is based on experimental results. The expression fit used in the Barrier code is

$$Y1 = \frac{(NumCycles - 50)}{((275 \cdot AIR) \cdot (1.0 + 0.43 \cdot AIR) \cdot F(WCR) - 100.0)} \quad (2)$$

where

$$F(WCR) = 4.2 - 8.0 \cdot WCR \cdot (1.0 - 0.4 \cdot WCR) \quad (3)$$

$Y1$ = the fractional decrease in dynamic modulus of elasticity of the concrete

N = number of freeze/thaw cycles

AIR = percent entrained air in the concrete

WCR = water-to-cement ratio.

$Y1 = 0.5$ is taken as the point of significant cracking and deterioration of the concrete due to freeze/thaw action. The amount of time (Tc) required to reach this level of damage is given by

$$T_c = (138 \cdot AIR)/N \cdot (1.0 + 0.43 \cdot AIR) \cdot F(WCR). \quad (4)$$

The annual rate of degradation (R_{fl}) is given by

$$R_{fl} = (N/T_c) \cdot \left(\frac{0.05}{\sqrt{(\theta)}} - 0.21 \cdot T_r \right) \quad (5)$$

where

θ = water content

T_r = residual water content (assumed = 0.09).

The Barrier code also computes the amount of time required to reach a given level of damage for a given value of fractional decrease in DME as well as an annual rate of concrete loss. The barrier data are, in part, based on the work of Pigeon et al. (1989).

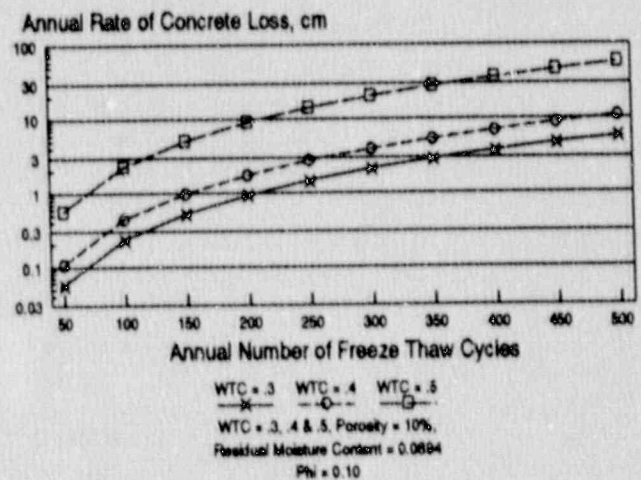An example of freeze/thaw loss predicted by the Barrier code equations is given in Figure 20.

Annual Rate of Concrete Loss, cm

WTC = .3, .4 & .5, Porosity = 10%,
Residual Moisture Content = 0.0684
Phi = 0.10

Figure 20. Loss from freeze/thaw damage with 7% entrained air.

CRACKING

Cracking can result from a number of phenomena including, drying shrinkage, temperature change stress, reinforcement corrosion with resulting expansion, carbonation, and physical loadings. The location and nature of a crack depends upon the cause. Current understanding of concrete cracking was summarized by an ACI committees (ACI, 1984, 1990).

The simplest form of crack is caused by physical loading on the roof of the structure. This leads to a set of partially penetrating cracks below the neutral axis of the slab (Figure 21). A lot of work has been done in predicting the location and size of cracks formed by physical loading of concrete beams and slabs (Broms, 1965; Bazant and Oh, 1983; Oh and Kang, 1987). A variety of formulae has been developed for crack prediction. In each case, the most important parameter is the amount of strain in the steel reinforcement.
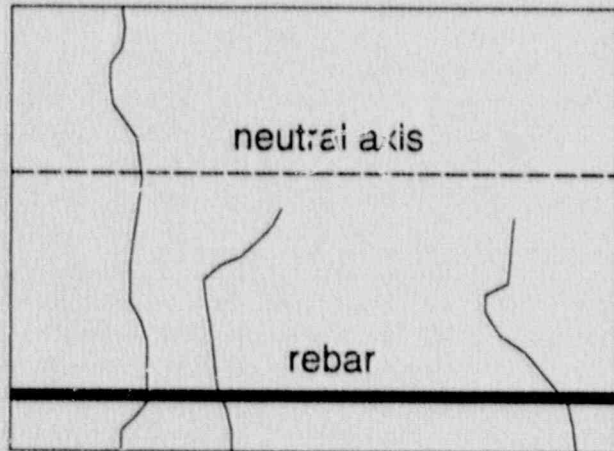
Figure 21. Schematic of cracks.

Microcracks in concrete may also be caused by drying shrinkage. As the concrete dries, the capillary pressure generated leads to shrinkage. Drying shrinkage leads to systems of parallel cracks that are usually too thin to be visible by the unaided eye (Bazant and Raftshol, 1982). This type of drying might occur during the operational period of a belowground vault. Even very tiny microcracks tend to dominate the permeability of the concrete at low pore water tensions.

Phenomena that cause general shrinkage of concrete, such as drying and carbonation, can lead to crack formation. Either drying shrinkage or carbonation can lead to shrinkage in the range of 0.08%, depending upon the moisture content at exposure. Combined, they can lead to 0.16% shrinkage. Lower moisture contents lead to greater drying shrinkage, whereas shrinkage from carbonation peaks at a relative

humidity of 50% (Verbeck, 1958). Temperature changes leading to swelling and shrinkage of the concrete also cause cracking.

Penetration Assumptions

One of the most crucial aspects of the evaluation of cracking is the assumption concerning penetration of the cracks. Most cracks from flexural loading are expected to penetrate only from the bottom of the roof to the neutral axis. Above the neutral axis, in the zone of compressive stress, most cracks would not be expected to penetrate. In the Barrier code (Shuman et al., 1989), cracks from physical loading are assumed initially to penetrate only to the neutral axis and not affect the hydrologic properties of the slab. Once the cracks reach a depth of three-fourths of the slab thickness or within 7.5 cm of the total slab thickness, they are assumed to fully penetrate the slab. The increased hydraulic conductivity caused by the crack is then added to the slab permeability in the form of an equivalent porous media. The specifics of the calculation of crack width, spacing, and unsaturated hydrologic properties in the Barrier code are not well documented.

Cracks resulting from volume changes in the concrete caused by temperature changes, drying shrinkage, and carbonation are more likely to penetrate the entire slab thickness. Penetration of the slab is facilitated by the absence of compressive forces at the top of the concrete slab.

Crack Prediction - Flexural Beams

The prediction of crack width and spacing in concrete flexural members has been the subject of a fair amount of research. The simplest expressions can be attributed to Broms (1965). Average crack spacing was given as

$$S_{avg} = 2t. \tag{1}$$

Average and maximum crack widths were given as

$$W_{avg} = 2t\epsilon,$$

$$W_{max} = 1.66W_{avg} \tag{2}$$

where

$\quad t \quad$ = concrete thickness over steel

$\quad \epsilon_s \quad$ = strain in the steel reinforcement

$\quad S \quad$ = crack spacing

$\quad W \quad$ = crack width at tension face.

Broms (1965) and Broms and Lutz (1965) made several observations concerning the nature of the cracks:

1. Primary tensile cracks could be observed on the surface of flexural members. The cracks extended to the neutral axis. Secondary tensile cracks were observed when the stress in the reinforcement reached approximately 20,000 - 30,000 psi. These cracks were confined to the immediate vicinity of the reinforcement. Longitudinal tensile cracks, which started at existing primary or secondary cracks and spread along the reinforcement, were noticed at the higher strain. Longitudinal cracks, which formed in the compression zone, were observed for the flexural members at high load levels.

2. "The surface crack width will be small if the reinforcement is distributed uniformly along the periphery of a member, if a large number of small diameter bars are used and if these bars are placed as close to the surface as feasible."

Bazant and Oh (1983) derived theoretical expressions for crack spacing in reinforced concrete. These expressions indicated good numerical agreement with the empirical Gergely-Lutz formula. Later Oh and Kang (1987) developed simpler, easier to use expressions for maximum crack width and crack spacing in concrete flexural members. These equations give a better fit to the data than the Gergely and Lutz formula.

The equations for maximum crack width are

$$\frac{W_{max}}{D} = a_0(\varepsilon_s - 0.0001)R \tag{3}$$

$$a_0 = 159\left(\frac{t_b}{h_2}\right)^{4.5} + 2.83\left(\frac{A_1}{A_{sl}}\right)^{1/3} \tag{4}$$

$$R = \frac{h_2}{h_3} \tag{4}$$

where

W_{max} = maximum crack width at extreme tension face

h_2 = distance between neutral axis and lower face

h_3 = distance between neutral axis and steel reinforcement center

A_1 = effective area of concrete surrounding one reinforcement bar

A_{sl} = area of one reinforcement bar

t_b = bottom concrete cover over reinforcement

D = reinforcement bar diameter

ε_s = steel strain.

To predict crack spacing, the following equation was used

$$\frac{s}{D} = c_0 + \frac{0.236 \times 10^{-6}}{\varepsilon_s^2}$$

$$c_0 = 25.7\left(\frac{t_b}{h_2}\right)^{4.5} + 1.66\left(\frac{A_1}{A_{sl}}\right)^{\frac{1}{3}} \tag{5}$$

where s is the average spacing of cracks. The average crack width at the surface using this formula would be

$$W_{avg} = s\varepsilon_s R. \tag{6}$$

These equations are especially convenient because of the dimensionless format.

Crack Prediction - Volume Change

Prediction of cracks caused by concrete volume changes is covered in ACI 207 (ACI, 1990). Volume change generally comes from temperature rise during setting, seasonal temperature variations, and drying shrinkage. In general, the summation of crack widths in a slab of concrete must balance the shrinkage minus the extension of the concrete. Cracks tend to originate at the midpoint between previous cracks. In simple geometries, this leads to a series of evenly spaced parallel cracks. Addition of steel reinforcement to the concrete tends to lead to smaller cracks with closer spacing. Thus the reinforcement is typically used to control the size and spacing of cracks. Smaller cracks are more likely to heal through autogeneous processes.

Autogenous Healing of Cracks

There is considerable evidence for autogenous healing of cracks formed in concrete (Guppy, 1988). Frequently, permeability of concrete has been found to decline with time in flow tests (Loadsman et al., 1988). Healing occurs from carbonation of calcium hydroxide in the cement paste by carbon dioxide. Calcium carbonate and hydroxide crystals are found to grow in the crack. Saturation of the crack with water appears to be essential for developing substantial strength from healing (ACI, 1984). Self healing is a very desirable property for materials utilized for radioactive waste isolation. The degree to which the self-healing properties of concrete can be "taken credit for" in quantitative performance assessments remains subject to question and is a fertile area for future research.

Implications of Cracking

Cracking has tremendous implications for performance of concrete barriers. Cracks represent a preferential pathway for fluid flow and mass transport that bypasses the favorable transport properties of the concrete matrix. In very small cracks, the primary resistance to fluid flow is the passage through the crack itself; however, in larger cracks the primary resistance to flow comes from entrance and exit head losses at the ends of the cracks. The entrance and exit

28

head losses are controlled by crack spacing and the permeability and thickness of the materials adjacent to the concrete. Frequently the leakage rate through a concrete slab will be directly proportional to the permeability of the adjacent soil or backfill. This fact suggests that low permeability backfill materials should be placed adjacent to concrete vaults if the impacts of cracking are to be minimized. The impacts of cracking on the performance of concrete barriers will be covered in a future NUREG document under the same FIN Number.

Radionuclide Geochemistry in Concrete

The geochemical environment of concrete in a LLW disposal setting affects not only the durability of the concrete but also the aqueous chemistry and transport properties of radionuclides that are released throughout the lifetime of a LLW disposal site. Because source term radionuclide concentrations are strongly dependent on the geochemical environment at the source, accurate and defensible modeling and performance assessment analyses of the release of radionuclides from (or through) concrete requires characterization of the temporal variation in concrete chemistry. There are also recent concerns about the radionuclide adsorption on colloids with subsequent transport. It is the combination of the physical and chemical properties of the concrete mixture together with the radionuclide properties that is responsible for radionuclide release and migration. This section briefly discusses the physical and chemical properties of concrete, the aqueous chemistry of pore fluids in concrete, the temporal variation in pore fluid chemistry within concrete, and the effects of concrete on the chemical behavior of earthen materials in a low-level disposal site. In addition, a discussion of the aqueous chemistry of important radionuclides in a concrete dominated system is presented.

Chemical and Physical Properties of Concrete

Concrete is composed of a mixture of cement, aggregate, water, and additives such as fly ash or silica flume. Because the chemistry of concrete is dominated by reactions that occur in the cement portion of the concrete, the focus of this section is on that chemistry. Portland cement is composed of primarily four compounds: tricalcium silicate (C_3S), dicalcium silicate (C_2S), tricalcium aluminate (C_3A), and tetracalcium aluminoferrite (C_4AF). During the curing of concrete, the cement hydrates to form a high surface area microporous matrix that is saturated with an aqueous phase. The composition of the aqueous phase assumes considerable importance in determining the properties of the composite (Angus and Glasser, 1985). Furthermore, the overall permeability and porosity of a concrete is dependent upon both the grain size of the hydrated cement paste and upon the grain size of any additives to the concrete. Because of the fine pore size, the transport and release of radionuclides in concrete will be dominated by diffusion as long as the

concrete is structurally intact. The physical properties of four types of concrete representative of barrier materials are given in Table 4.

Table 4. Properties and constituents of example concretes (Jakubick *et al.*, 1987).

	Normal Density - ND with fly ash	High Density - HD with silica fume
Properties		
Compressive Strength (28 days), MPa	42.0-29.9	39.0-62.6
Porosity, Vol. %	12.8-12.4	9.6-6.5
Hydraulic Conductivity (m/s)	3.2×10^{-10}- 4.9×10^{-10}	3.9×10^{-10}- 7.0×10^{-10}
Density (kg/m^3)	2593-2‍18	4036-3894
Composition, Vol. %		
Course Aggregate	38.4-43.3	40.4-40.7
Fine Aggregate	30.5-30.0	27.3-27.5
Fly Ash	0.3	
Silica Fume		3.7
Cement	12.1-8.6	12.9-10.4
Water	15.6-14.1	1.50-11.4
Voids	3.4	4.4-6.3

The microporous matrix phase of Portland cements (sulfate free) contains a poorly crystalline to amorphic calcium silicate hydrate (C-S-H) gel and crystalline $Ca(OH)_2$ (portlandite). Although C-H-S exhibits considerable short-range ordering, it is X-ray amorphous because long range ordering is minimal (Grutzek, 1989). C-H-S also exhibits extensive solid solutions and can be formulated as $Ca_xH_{6-2x}Si_2O_7 \cdot zCa(OH)_2 \cdot nH_2O$ (Glasser, 1987). In addition, the occurrence of aluminates in unhydrated cement results in the formation of silica substituted hydrogarnet (Grutzeck, 1989). The occurrence of alkali oxides (Na_2O and K_2O) in the unhydrated cement dominates the aqueous chemistry of new concrete as discussed below (Angus and Glasser, 1985). The chemical composition of typical cement is given in the Table 5.

Table 5. Chemical composition limits of Portland cements (Neville, 1981).

Oxide	Wt. percent
CaO	60 - 67
SiO_2	17 - 67
Al_2O_3	3 - 8
Fe_2O_3	0.5 - 6.0
$Na_2O + K_2O$	.02 - 1.3
SO_3	1 - 3
MgO	0.1 - 4

Concrete Pore Water Chemistry

The hydration of cements results in the formation of very alkaline pore fluids. It had been believed that the solubility of portlandite controlled the pH of pore fluids. However, Glasser et al. (1985) indicate that direct analysis of pore fluids reveals that NaOH and KOH are the dominate electrolytes (Table 6); all other things being equal, the alkali concentrations and the pH of pore fluids are a function of the alkali content of the cement. Since much of the alkali present in cement is rapidly released to the pore fluids (Glasser et al., 1985), the importance of alkali hydroxides in the pore fluid will be temporary. Leaching of the cement by groundwater results in the loss of alkalis, and the pH of the pore fluid drops as portlandite and C-S-H reactions become important. The early presence of alkalis is unbuffered; once they have been leached from the pore fluid, there is no mechanism to replace them. C-S-H reactions are buffered by the solubility of phases in the hydrated cement. For systems open to the transport of chemical species by groundwater, irreversible reactions will occur in the concrete. An example of such a reaction is the altering of portlandite to calcite by CO_2 dissolved in groundwater via

$$Ca(OH)_2 + 2HCO_3^- = CaCO_3 + H_2O + CO_3^{2-}. \qquad (1)$$

Reactions, such as above, coupled with physical displacement of pore water by diffusion dominated transport results in a gradual loss of buffering capacity. This loss can be visualized as a series of stages with the pH gradually dropping over time (Atkinson et al., 1988). Because of fluid flow though the disposal site, the expected pH drop will not be uniform. Atkinson (1985) estimates a range of from approximately 10^4 years for the pH to drop to less than 10.5 in the outer meter of a highly permeable concrete disposal facility in contact with a groundwater, containing reactive species to 2×10^7 years at the center of a disposal facility. An example of the temporal variation of pH for a groundwater containing reactive ionic species is shown in Figure 22. In general, the processes that lower the pH in the concrete are very slow, requiring time periods on the order of thousands or millions of years for completion. These results suggest that the influence of concrete on the chemical environment of the disposal facility may last for hundreds of thousands of years. Hence, the chemical effects of concrete can far outlast the structural lifetime of the concrete.

Reduction in pH when Affected by Groundwater Containing 0.01 Mole of "Reactive" Ions
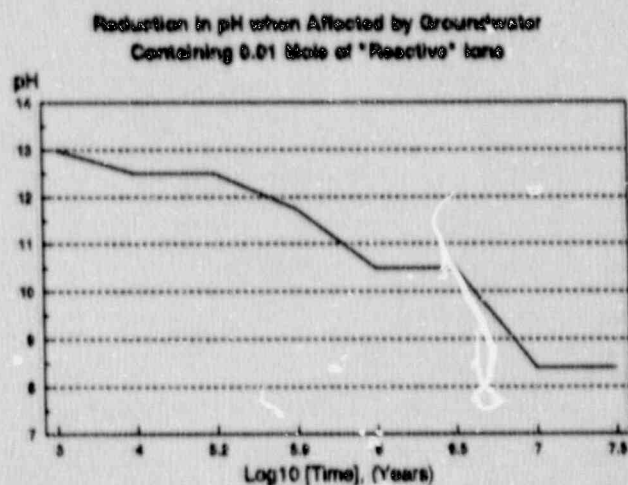
Figure 22. Change in pH with time as predicted by Atkinson et al., 1987.

The redox chemistry of concrete is controlled primarily by additives to the cement. Angus and Glasser (1985) found that the Eh of blastfurnace slag (BFS) cement was slightly oxidizing (+35 to +82 mV) and insensitive to composition for OPC:BFS ratios above 0.33. For lower ratios, reducing Eh values as low as -330 mV were observed. However, the addition of zinc or magnesium powder to OPC had no effect on Eh. Tuutti (1982) suggests that nonpassivated mild steel will lower the Eh of pore waters. Eh values of pore water provide insight into the potential redox speciation of radionuclides. However, the long term chemical performance of cement is also a function of its reducing capacity. The reported reducing capacity of BFS is 1.1 mmole g^{-1} and compares to values of 0.1 mmole g^{-1} for OPC and 0.2 for high alumina cement and natural pozzolan (Angus and Glasser, 1985). These results suggest that concrete can be engineered to have pore water Eh values that will ensure that radionuclides with multiple oxidation states (e.g., plutonium) are reduced.

Angus and Glasser (1985) also found that the BFS altered the aqueous speciation of sulfur. For a OPC:BFS ratio of lower than 0.33, aqueous sulfide concentrations of 4 to 34 mmole liter^{-1} were observed by Angus and Glasser (1985). The presence of sulfide in pore water may limit the concentration of radionuclides that are chalcophile elements (e.g., cobalt) by the formation of insoluble sulfide phases.

Table 6. Measured ranges of pore-water compositions of hydrated cements (Berner, 1987). Composition in mmole liter[-1] except for Eh (mV) and pH.

	Oxidizing[a]	Reducing[b]
Na	13-70	78-139
K	15-200	146-154
Ca	0.4-12	0.5-2.3
Mg	0 - 0.01	<0.01
Si	<0.2	0-0.2
pH	84-139	-377 - -196

a. Based on six cements. b. Based on two cements.

Modification of External Environment by Concrete

The alkaline cement components that leach from the concrete may have a significant influence on the earthen materials surrounding the concrete barrier. Jefferies et al. (1988) investigated the response of clays in contact with concrete. They found that the buffering capacities of clays subject to alkali intrusion are best explained by cation exchange of aqueous calcium for sorbed cations and the precipitation of calcite. The saturation of the clay with calcium and the precipitation of calcite may affect the sorptive and hydraulic properties of the clays. Jefferies et al. (1988) also state that the pH of clay pore waters will ultimately rise to about 12 because of the long term chemical effects of concrete.

The importance of the potential changes to the surrounding materials depends upon the aspect of performance considered. Dispersion and expansion of clays leads to filling gaps and fissures in the system and lowers hydraulic conductivity but results in lower slope and structural stability. The precipitation of calcite "cement" in clay materials may lead to hardening and embrittlement of the clay. In addition, Melchoir et al. (1988) suggest that mineral phase transformation in earthen materials as a result of interactions with concrete needs to be considered.

The affects of pH on the sorptive properties of radionuclides on clinoptilolite and Dochart clay have been investigated by Buckley, Philipose et al. (1988). Their results are shown in Figures 23 and 24.
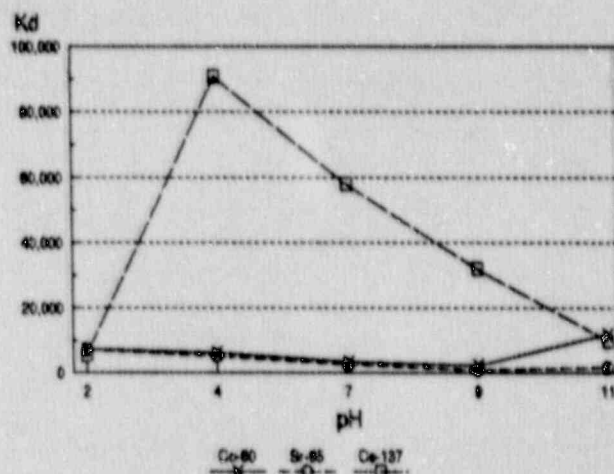
Figure 23. Effect of pH on distribution coefficient of conditioned clay (Buckley et al., 1988).
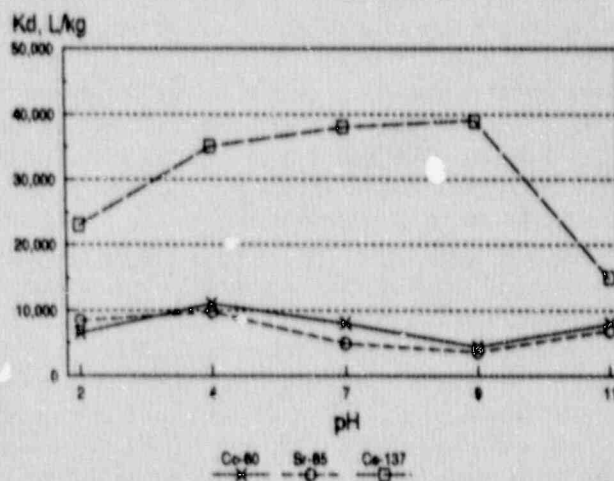
Figure 24. Effect of pH on distribution coefficient of conditioned clinoptilolite (Buckley et al., 1988).

Radionuclide Behavior

The radionuclides used to classify waste types in 10 CFR 61 are taken as a starting point for selection of the radionuclides of interest. The primary selection criteria of the regulations are based on radionuclide lifetime and imminent hazard such as reactivity and high probability of uptake to living organisms and humans. Other criteria in addition to these include: expected disposal site environment; radionuclide inventory level; disposal facility performance effects; chemical state; and radioactive progeny. The basis for selection needs further examination. Relative to concrete performance in particular, certain radionuclides, or chemicals in the waste or groundwater, of high chemical reacti. ity, concentration, and sufficient lifetime could be detrimental to a concrete disposal facility and its concrete components. Reported results from the literature are given below for the radionuclides of interest in LLW.

32

The aqueous chemistry of radionuclides and other contaminants in concrete will be dominated by the interactions of portlandite, C-S-H, and additives with the pore fluids. As discussed, the pore fluids are characterized by high pH values and oxidizing to reducing Eh values. The concentrations of common inorganic ligands in the pore-fluids are reduced because of the high pH and calcium concentrations. Carbonate is likely to be removed from ingressed groundwater by the precipitation of calcite. Likewise, phosphate is reduced by the precipitation of apatite $[Ca_5(PO_4)_3OH]$ or other insoluble phosphates. The predominate ligands in pore fluid are hydroxide, sulfur species (SO_4^{2-}, $S_2O_3^{2-}$, and HS^-), and perhaps chloride.

Carbon and Carbon-14. Carbon-14 has a half-life of 5,730 years and is easily taken up into the biosphere in solid, liquid, or gaseous compounds. Carbon combines with many other elements to give solid or highly mobile, liquid or gaseous compounds. It is also a primary constituent of living matter. The aqueous chemistry of carbon for disposal facility condition will be dominated by carbonate equilibria. Hietanen et al. (1985) found that carbon-14 was effectively removed from the aqueous phase in groundwater/concrete tests by the precipitation of calcium carbonate.

Iodine and Iodine-129. Iodine-129 has a half-life of 15.7 million years and is also easily taken up into the biosphere. In humans, iodine is an important chemical in the endocrine system and thyroid. For all but the most oxidizing conditions, iodide (I^-) will be the predominate form of iodine in pore fluids and groundwater. Iodine is more strongly sorbed to hydrated cement than to natural silicates (Höglund et al., 1985), and I^- will be less mobile in concrete than in neighboring geologic media. Atkins and Glasser (1990) studied the adsorption properties of specific phases in concrete. They found that OPC is a good adsorbent for I^- and that the hydrate calcium aluminum sulfates were the best sorbents. The Atkins and Glasser result provides insight into the Hoeglund et al. (1985) observation that the sorption of iodine on BFS cements was lower than for other cements. Because BFS cements are more reducing, significant portions of the sulfate is reduced to sulfide resulting in smaller amounts of hydrate calcium aluminum sulfates.

Actinides. The aqueous chemistry of actinide elements (of interest here are thorium, uranium, neptunium, plutonium, and americium) is characterized by a multiple oxidation state. The behavior of actinides in concrete pore-fluids will be strongly influenced by the Eh. The aqueous chemistry will be dominated by the formation of neutral or anion hydroxide complexes (Allard, 1983). Höglund et al. (1985) report high sorption and low mobility of actinides in pore fluid/concrete systems. They also observed that the sorption behavior (as measured by K_d) is very similar for trivalent (Am), tetravalent (Th), pentavalent

(Np), hexavalent (U), and mixed valent (Pu) actinides. These results suggest that concrete can be an extremely effective barrier to actinide migration.

Hydrogen and Tritium. Hydrogen-3, tritium has a half-life of 12.3 years and can replace hydrogen in most of its compounds. Tritium is very mobile in most circumstances, and because it is present as tritiated water, it will not interact significantly with water saturated concrete. Uncoated concrete absorbs water rapidly, and once wetted, conducts tritium in the waters at about 8×10^{-4} cm^3 cm^{-2} day^{-1} (Eichholz et al., 1989). Diffusion rates can be reduced by finishing the concrete surface or using a smaller aggregate size and vibratory packing. Unless a concrete wall is coated or sealed in some way, little credit can be taken for concrete as a retarding barrier (Eichholz et al., 1989). Harris (1988) reports that the transport of tritium is not hindered by concrete.

Technetium and Technetium-99. Technetium 99 has a half-life of 2.6 million years and in oxidized form (TcO_4^-) is highly soluble and easily taken up in the biosphere. The aqueous chemistry of technetium in concrete pore fluids can be very complex because for oxidizing conditions, the highly soluble pertechnetate ion dominates. Tallent et al., (1988) investigated the behavior of pertechnetate and nitrate in BFS cement-based materials. They found that the inclusion of BFS reduced the release of technetium but not nitrate and attribute this difference to reduction of pertechnetate to the tetravalent oxide. Lee and Bondietti (1983) indicate that ferrous iron or sulfide bearing waters decrease the mobility of technetium by precipitating reduced technetium bearing iron and sulfide phases. These results suggest that technetium can be effectively retarded by engineering the chemical properties of concrete barriers.

Cobalt and Cobalt-60. Cobalt-60 has a half-life of 5.3 years and can become resident in bone structures. Cobalt occurs as anionic hydroxide species in pore fluids (Baes and Mesmer, 1976). Cobalt (II) hydroxide has a minimum solubility in the pH range of 10.2 to 11.5. The concentration of cobalt in pore fluids may be suppressed further by substituting for calcium in portlandite and C-S-H. Habayeb (1985) found that release of cobalt-60 from cement waste forms was below detection levels.

Strontium and Strontium-90. Strontium-90 has a half life of 28.5 years, readily replaces calcium in carbonate compounds, and becomes resident in bone structures. Strontium is retarded by BFS concretes (Harris, 1988). In concrete pore fluids, strontium will occur as Sr^{2+} and $Sr(OH)^+$. Because of the similarities between calcium and strontium, theses two ions compete for similar sites and ligands in concrete. Therefore, the sorption/precipitation of strontium is a function of the Ca:Sr ratio of the fluid. Jakubick et al. (1987) found that the sorption of strontium onto concrete is greater for sodium chloride solution than

for calcium chloride solutions. In addition, during calcite precipitation, strontium is preferentially enriched in the fluid phase relative to calcium (Mucci and Morse, 1983). Sorption experiments with concrete indicate that strontium is only weakly adsorbed (Jakubick et al., 1987; Hietanen et al., 1985).

Cesium and Cesium-137. Cesium-137 has a half-life of 30 years. Hoyle and Grutzeck (1988) incorporated cesium hydroxide in cement and observed complete removal of cesium from a solution in the form of cesium zeolites. They also observed that cesium fixation increased as the amount of calcium decreased and the ratio of Al:Si increased. Grutzeck (1989) reports that the concrete phases that form affect the chemistry of the remaining pore solution and tailoring concrete with silica or BFS can reduce the pore solution composition of cesium and strontium by a factor of 10. Furthermore, decreasing the activity of the calcium in the system led to a decrease in the amount of cesium and strontium leached by a factor of ten. Hietanen et al. (1985) found high sorption of cesium in tests made with natural ground waters. However, the sorption of cesium on concrete is due primarily to adsorption on the aggregate. Robertson (1984) notes preferential sorption of Cesium-137 and Cesium-134 on unfinished or eroded concrete surfaces used in reactors. The behavior of cesium in concrete is compositionally dependent, with the formation of cesium bearing zeolitic phases limiting cesium mobility.

Summary

Concrete acts as a effective barrier for the migration of most radionuclides. The potential problem nuclides are tritium, iodine, strontium, technetium, and cesium. Design consideration of the chemical environment in concrete can result in substantial improvement of concrete as a barrier to radionuclide migration. The mobility of radionuclides can be reduced in most cases by a factor of 10 and in some cases by a factor of 100. The transport and release of radionuclides in concrete will be primarily by diffusion as long as the concrete is structurally intact. Longer curing (Crawford et al., 1985) or the custom tailoring of concrete can achieve reduced permeability and porosity, reduced leachability, lower diffusion rates, and increased sorption for most radionuclides (Harris, 1988; Grutzeck, 1989; Izumida et al., 1987).

SUMMARY AND CONCLUSIONS

This report has summarized and critically evaluated some of the models available for estimating long-term degradation of concrete barriers. A companion report will evaluate the implications of degradation on fluid flow and mass transport through concrete barriers. It is apparent that available models are limited in terms of scope and validity. Although more sophisticated models are continuously being developed, all the inherent problems will not be resolved soon. Several problem areas are discussed below.

Concrete longevity is dependent upon quality, much more so than most materials. This high dependence on the quality of cement; aggregate type, size, and quantity; water-to-cement ratio; and workmanship severely limits our ability to quantitatively estimate performance. A simple example comes from the building where one of the authors works. Outside the back door are two rain spouts constructed from concrete. In the approximately 5 years the building has been in existence, one of the rain spouts evidences no visual damage while the other spout has completely degenerated into a rubble heap. Although quality assurance levels can be expected to be much higher in LLW disposal facility construction, leading to more consistent concrete quality, the observation nonetheless illustrates the potential problems with predicting long-term concrete performance.

The sections on individual types of concrete attack do not address the combined or coupled effect of all processes working simultaneously. In the Barrier code (Shuman et al., 1989), the coupled attack is simulated with annual changes in the properties of each concrete layer. Processes such as sulfate attack and freeze/thaw are assumed to lead to annual reductions in the effective thickness and transport properties of the concrete slab. For example, a loss in thickness of the outer roof surface translates into a reduction in the steel reinforcement cover thickness, causing more rapid initiation of corrosion. Since most of the empirical concrete degradation models were based upon data from a single type of attack on concrete samples with fixed dimensions, the approach is not necessarily valid in all cases. However, in the absence of more detailed information, this may be the best available option. The coupling approach applied in the Barrier code is at least more conservative (i.e., predicts more rapid degradation) than separate applications of each degradation model, such as the example calculations included at the end of most sections in this document.

The models that currently exist have almost entirely been derived from the point of view of external attack. Prediction of attack rates from materials included in the wastes will be made more difficult by the absence of appropriate models.

Our ability to model concrete performance is limited on all sides. The empirical concrete degradation models included in this report are of necessity applied outside their range of validity when evaluating long-term performance of concrete. Mechanistic models, where available, frequently lack adequate parameter data bases. In some cases, the mechanistic models predict trends that directly conflict with experimental and historical data.

The lack of adequate models and physical understanding for many of the degradation processes makes the application of Monte-Carlo and other statistical techniques to account for uncertainty of questionable validity. Statistical techniques that propagate parameter uncertainties cannot account for basic uncertainties or lack of understanding in the conceptual model of the waste isolation system. Given the current state of model development, the classical conservative analysis mode of calculations may be most appropriate.

Cracking of the concrete is one of the most difficult types of degradation because it is very difficult to predict where and when cracks will occur. Although predictive models are available for cracking in simple structural arrangements (e.g., flexural beams), their application to complex underground structures over long time periods remains questionable. The difficulty of predicting crack occurrence must then be combined with significant changes to permeability of the concrete. Even a very small crack can change the transport properties of a concrete slab by orders of magnitude. After formation, the cracks may self heal over time, although the specifics of when autogenous healing will occur are not clear. In cases where crack formation is not expected, it is difficult to clearly demonstrate in a performance assessment that no cracks will form. Questions such as the following are of prime importance to understanding and predicting the long-term performance of concrete barriers: When and where will cracks occur?, Under what conditions does autogenous healing occur?, and What is the impact of cracks upon performance of the concrete barrier? A future publication will analyze the impact of cracking on concrete performance.

The geochemical properties of concrete offer great promise because they are long lasting and robust, and concrete chemistry shows promise for significant retardation of carbon and iodine, two radionuclides that are difficult to contain.

Further development work is needed in all areas of concrete degradation. A major priority should be in the analysis of cracking and autogenous healing of cracks. Cracking is the one degradation process that is most difficult to predict and can have the greatest impact upon performance.

BIBLIOGRAPHY

American Concrete Institute Committee 222, "Corrosion of Metals in Concrete," *ACI Journal*, p. 3-32, January - February, 1985.

American Concrete Institute Committee 224, "Causes, Evaluation, and Repair of Cracks in Concrete Structures," *ACI Journal*, p. 211-230, May-June, 1984.

Alcorn, S. R., J. Myers, M. A. Gardiner, and C. A. Givens, "Chemical Modeling of Cementitious Grout Materials Alteration in HLW Repositories," *Waste Management 89*, University of Arizona, p. 279-286, 1989.

Alford, N. McN., and A. A. Rahman, "An Assessment of Porosity and Pore Sizes in Hardened Cement Pastes," *Journal of Materials Science, 16*, p. 3105-3114, 1981.

Allard, B. (1983) *Actinide Solution Equilibria and Solubilities in Geologic Systems*, SKBF/KBS Teknisk Rapport 83-35, Svensk Kärnbränslefösörjning AB / Avdelning KBS, Stockholm, Sweden.

Angus, M.J. and Glasser, F.P., "The Chemical Environment in Cement Matrices, Scientific Basis for Nuclear Waste Management VII," *Materials Research Society Reseach Symposium Proceedings, 50*, p. 547-556, 1985.

Atkins, M., and F.P. Glasser, "Encapsulation of Radioiodine in Cementitious Waste Forms," *Materials Research Society, 176*, p. 15-22, 1990.

Atkinson, A., *The Time Dependence of pH Within a Repository for Radioactive Waste Disposal*, AERE Harwell Report No. DOE/RW/85.062, 1985.

Atkinson, A., A. K. Nickerson, and T. M. Valentine, "The Mechanism of Leaching From Some Cement-Based Nuclear Wasteforms," *Radioactive Waste Management and the Nuclear Fuel Cycle, 4(4)*, p. 357-378, 1984.

Atkinson, A., and J. A. Hearne, *An Assessment of the Long-Term Durability of Concrete in Radioactive Waste Repositories*, AERE-R11465, Harwell, U.K., 1984.

Atkinson, A., D. J. Goult, and J. A. Hearne, "An Assessment of the Long-Term Durability of Concrete in Radioactive Waste Repositories," *Materials Research Society, 50*, p. 239-246, 1985.

Atkinson, A., F.T. Ewart, S.Y.R. Pugh, H.H. Rees, S.M. Sharland, P.W. Tasker, and J.D. Wilkins, "Experimental and Modeling Studies of the Near-field Chemistry for Nirex Repository Concepts", *Near-Field Assessment of Repositories for Low and Medium Level Radioactive Waste*, Nuclear Energy Agency, OECD, Paris, p. 143-157, 1988.

Atkinson, A. and J. A. Hearne, "Mechanistic Model for the Durability of Concrete Barriers Exposed to Sulphate-Bearing Groundwaters," *Materials Research Society, 176*, p.149-156, 1990.

Atkinson, A. and A. K. Nickerson, "Diffusion and Sorption of Cesium, Strontium, and Iodine in Water-Saturated Cement," *Nuclear Technology, 81*, p. 100-113, 1988.

Baes, C.F., and R.E. Mesmer, *The Hydrolysis of Cations*, Wiley Interscience, New York, pp. 489, 1976.

Bazant, Z. P., J. Chern, A. M. Rosenberg, and J. M. Gaidis, "Mathematical Model for Freeze-Thaw Durability of Concrete," *J. Am. Ceram. Soc., 71(9)*, p. 776-783, 1988.

Bazant, Z. P., "Physical Model for Steel Corrosion in Concrete Sea Structures - Theory," *ASCE Structural Division Journal, 105(6)*, p. 1137-1153, 1979a.

Bazant, Z. P., "Physical Model for Steel Corrosion in Concrete Sea Structures - Application," *ASCE Structural Division Journal, 105(6)*, p. 1155-1166, 1979b.

Bazant, Z. P. and B. H. Oh, "Spacing of Cracks in Reinforced Concrete," *ASCE Journal of Structural Engineering, 109(9)*, p.2066 - 2085, 1983.

Bazant, Z. P. and W. J. Raftshol, "Effect of Cracking in Drying and Shrinkage Specimens," *Cement and Concrete Research, 12*, p. 209-226, 1982.

Broms, B. B, and L. A. Lutz, "Effects of Arrangement of Reinforcement on Crack Width and Spacing of Reinforced Concrete Members," *Journal Amer. Concrete Institute, 10*, p. 1395 - 1409, 1965.

Broms, B. B., "Crack Width and Crack Spacing in Reinforced Concrete Members," *Journal Amer. Concrete Institute, 10*, p. 1237 - 1255, 1965.

Buckley, L.P., Philipose, K.E. and Torok, J., "Engineered Barriers and Their Influence on Source Behavior", IAEA Conference Proceedings on: Management of Low and Intermediate Level Radioactive Wastes, *1*, p. 147-161, 1988.

Clear, K. C., *Time to Corrosion of Reinforcing Steel in Concrete Slabs, Vol. 3. Performance Agter 830 Daily Salt Applications*, Federal Highway Administration Report No. FHWA-RD-76-70, NTIS PB-258 446, 1976.

Clifton, J. R., *The Frost-Resistance of Concrete*, NISTIR 90-4229, National Institute of Standards and Technology, 1990.

Codell, R. B. and J. D. Duguid, "Transport of Radionuclides in Groundwater," J. E. Till and H. R. Meyer ed., *Radiological Assessment: A Textbook on Environmental Dose Analysis*, NUREG/CR-3332, 1983.

Crank, J., *The Mathematics of Diffusion*, Oxford University Press, Oxford, 1975.

Crawford, R.W., F.P. Glaser, A.A. Rahman, M.J. Angus, and C.E. McCulloch, "Diffusion Mechanisms and Factors Affecting Leaching of Caesium-134 from Cement Based Waste Matrices," *Radioactive Waste Management and the Nuclear Fuel Cycle*, 6, p. 177-196, 1985.

Daian, J., "Condensation and Isothermal Water Transfer in Cement Mortar, Part I - Pore Size Distribution, Equilibrium Water Condensation and Imbibition," *Transport in Porous Media*, 3, p. 563-589, 1988.

Detwiler, R. J., B. J. Dalgleisch, and R. B. Williamson, "Assessing the Durability of Concrete in Freezing and Thawing," *ACI Materials Journal*, p. 29-35, 1989.

Eichholz, G.G., Park, W.J., and Hazin, C.A., "Tritium Penetration Through Concrete," *Waste Management*, 9, p. 27-36, 1989.

Glasser, F.P., M.J. Angus, C.E. McCulloch, D. Macphee, and A.A. Rahman, "The Chemical Environment in Cements," *Materials Research Society*, 44, p. 849-858, 1985.

Grutzek, M.W., *Physical Chemistry of Portland Cement Hydrate, Radioactive Waste Hosts*, US DOE Report No. DOE/ER/45145--4, January 1989.

Guppy, R., *Autogenous Healing of Cracks in Concrete and its Relevance to Radwaste Repositories*, NSS/R-105, DE88 753994, Nirex, United Kingdom, 1988.

Habayeb, M.A., "Leaching Performance of Cemented Decontamination Wastes," *Nuclear and Chemical Waste Management*, 5, p. 305-314, 1985.

Harker, A. H., S. M. Sharland, and P. W. Tasker, "A Mathematical Model of Uniform Corrosion of Intermediate Level Radioactive Waste Canisters in Concrete," *Radioactive Waste Management and the Nuclear Fuel Cycle*, 8(1), p. 65-85, 1987.

Harris, A.W., A. Atkinson, A.K. Nickerson, and N.M. Everitt, *Mass-Transfer in Water Saturated Concretes*, Safety Studies Nirex Radioactive Waste Disposal, NSS/R125, Harwell Laboratory, Didcot, Oxon, UK, 1988.

Harrison, W. H., and D. C. Teychenné, *Sulphate Resistance of Buried Concrete: Second Interim Report on Long Term Investigation at Northwick Park*, Building Research Establishment, Her Majesty's Stationery Office, London 1981.

Hem, J. D., *Study and Interpretation of the Chemical Characteristics of Natural Water*, USGS Water-Supply Paper, pp. 1473, 1970.

Hietanen, R., T. Jaakola, and J.K. Miettinen, "Sorption of Cesium, Strontium, Iodine and Carbon in Concrete and Sand," *Materials Research Society*, 44, p. 891-898, 1985.

Hillel, D., *Soil and Water Physical Principles and Processes*, Academic Press, New York, 1971.

Höglund, S., L. Eliasson, B. Allard, K. Andersson, and B. Torstenfelt, "Sorption of Some Fission Products and Actinides in Concrete Systems," *Materials Research Society*, 50, p. 683-690, 1985.

Horne, R. A., *The Chemistry of Our Environment*, Wiley Interscience, New York, 1978.

Hoyle, S.L. and M.W. Grutzek, "Fixation of Cesium by Calcium Aluminosilicate Hydrates," *Materials Research Society Reseach Symposium Proceedings*, 112, p. 13-21, 1988.

Izumida, T. F. Kawamura, K. Chino, and M. Kikuchi, "Stability of Cement-Glass Packages Containing Borate Salt Generated from Pressurized Water Reactor Power Plants," *Nuclear Technology*, 78, p. 185-190, 1987.

Jakubick, A. T., R. W. Gillham, I. Kahl, and M. Robin, "Attenuation of Pu, Am, Cs and Sr Mobility in Concrete," *Materials Research Society*, 84, p. 355, 1987.

Jefferies, N. L., C. J. Tweed, and S. J. Wisbey, "The Effects of Changes in pH Within a Clay Surrounding a Cementitious Repository," *Mat. Res.*, 112, p. 43-52, 1988.

Klieger, P., "Durability Studies at the Portland Cement Association," *Durability of Building Materials and Components*, ASTM STP 691, P.J. Sereda and G.G. Litvan, Eds., American Society of Testing and Materials, p. 282-300, 1980.

Laney et al., *Subsurface Investigations Program at the Radioactive Waste Management Complex of the Idaho National Engineering Laboratory, Annual Progress Report: FY-1987*, DOE/ID-10183, 1988.

Lea, F. M., *The Chemistry of Cement and Concrete*, 3rd Edition, Edward Arnold Ltd., London, 1970.

Lee, Y.S., and Bondetti, E.A., "Technetium Behavior in Sulfide and Ferrous Iron Solutions," *Materials Research Society*, 15, p. 315-322, 1983.

Likens, G. E., F. H. Bormann, R. S. Pierce, J. S. Eaton, and N. M. Johnson, *Biogeochemistry of a Forested Ecosystem*, Springer-Verlag, New York, 1977.

Loadsman, R. V. C., D. H. Acres, C. J. Stokes, and L. Wadeson, *A Study of the Water Permeability of Concrete Structures*, DOE Report No: DOE/RW/88052, United Kingdom, 1988.

Melchior, D., R. Glazier, and R. Marton, "Geochemical Performance of Earthen and Cementitious Sealing Materials for Radioactive Waste Repositories," *Waste Management '88*, University of Arizona, p. 745 - 751, 1988.

Mucci, A., and J.W. Morse, "The incorporation of Mg^{2+} and Sr^{2+} into Calcite Overgrowths: Influences of Growth Rate and Solution Composition," *Geochim. Cosmochim. Acta, 47*, 217-233, 1983.

Neville, A. M., *Properties of Concrete, 3rd Edition*, John Wiley & Sons, New York, 1981.

Newman, J., *Electrochemical Systems*, Prentice Hall, New Jersey, 1973.

Oh, B. H. and Y-J Kang, "New Formulas for Maximum Crack Width and Crack Spacing in Reinforced Concrete Flexural Members," *ACI Structural Journal*, p. 103-112, March-April, 1987.

Papadakis, V. G., C. G. Vayenas, and M. N. Fardis, "A Reaction Engineering Approach to the Problem of Concrete Carbonation," *AIChE Journal, 35(10)*, p. 1639-1650, 1989.

Pigeon, M., and M. Lachance, "Critical Air void Spacing Factors for Concretes Submitted to Slow Freeze-Thaw Cycles," *ACI Journal*, p. 282-290, 1981.

Pigeon, M., J. Prevost, and J. Simard, "Freeze-Thaw Durability Versus Freezing Rate," *ACI Journal*, p. 684-692, 1989.

Portland Cement Association, *Effects of Substances on Concrete and Guide to Protective Treatments*, PCA Publication IS001.0T6, 1986.

Powers, T. C., *A Hypothesis on Carbonation Shrinkage*, PCA Research Department Bulletin 146, 1962.

Powers, T. C., *Physical Properties of Cement Paste*, PCA Research Department Bulletin 154, 1960.

Powers, T. C., "Structure and Physical Properties of Hardened Portland Cement Paste," *Journal American Ceramic Society*, 41(1), p. 1-6, 1958.

Rasmuson, A., I. Neretnieks, and M. Zhu, "Calculations of the Degradation of Concrete in a Final Repository for Nuclear Waste" *Proceedings of an NEA Workshop on Near-Field Assessment of Repositories for Low and Medium Level Radioactive Waste, Baden, Switzerland*, 1987.

Robertson, D.E., K.H. Abel, C.W. Thomas, E.A. Lepel, W.V. Thomas, L.C. Carrick, M.W. Leale, and J.C. Evans, "Residual Radionuclide Contamination With and Around Nuclear Power Plants: Origins, Distribution, Inventory and Decommissioning Assessment" *Radioactive Waste Management and the Nuclear Fuel Cycle 5*, 285-310, 1984.

Shuman, R., V. C. Rogers, and R. A. Shaw, "The Barrier Code for Predicting Long-Term Concrete Performance," *Waste Management 89*, University of Arizona, 1989.

Stark, D., *Longtime Study of Concrete Durability in Sulfate Soils*, PCA SP-77, 1982.

Subramanian, E. V., and H. G. Wheat, "Depassivation Time of Steel Reinforcement in a Chloride Environment - A One-Dimensional Solution," *Corrosion, 45(1)*, p.43-48, 1989.

Tallent, O.K., E.W. McDaniels, C.D. Del Cul, K.E. Dodson, and D.R. Trotter, "Immobilization of Technetium and Nitrate in Cement-based Materials," *Materials Research Society, 112*, p. 23-32, 1988.

Turnbull, A., *British Corrosion Journal, 15(4)*, 1980.

Tuutti, K., *Corrosion of Steel in Concrete*, Swedish Cement and Concrete Research Institute, Stockholm, 1982.

Verbeck, G. J., *Carbonation of Hydrated Portland Cement*, PCA Research Department Bulletin 87, 1958.

Walton, J. C., and B. Sagar, "A Corrosion Model for Nuclear Waste Containers," *Scientific Basis for Nuclear Waste Management X*, Materials Research Society, *84*, p. 271 - 282, 1987.

Walton, J. C., and B. Sagar, "Modeling Performance of Steel Containers in High-Level Waste Repository Environments: Implications for Waste Isolation," *Radioactive Waste Management and the Nuclear Fuel Cycle*, Vol. *9(4)*, p. 323-347, 1988.

Wang, J. S. Y. and T. N Narasimhan, "Hydrologic Mechanisms Governing Fluid Flow in a Partially Saturated, Fractured, Porous Medium," *Water Resour. Res., 21(12)*, p. 1861-1874, 1985.

Wosten, J. H. M. and van Genuchten, M. Th. Using texture and other soil properties to predict the unsaturated soil hydraulic functions, *Soil Sci. Soc. Am Journal, 52*, p. 1762-1770, 1988.

Yonezawa, T., V Ashworth, and P. M. Procter, Pore Solution Composition and Chloride Effects on the Corrosion of Steel in Concrete *Corrosion, 44(7)*, p. 489-499, 1988.

2. TITLE AND SUBTITLE

Models for Estimation of Service Life of Concrete Barriers in
Low-Level Radioactive Waste Disposal

3. DATE REPORT PUBLISHED

MONTH	YEAR
September	1990

4. FIN OR GRANT NUMBER

A6858

5. AUTHOR(S)

J. C. Walton, L. E. Plansky, R. W. Smith

6. TYPE OF REPORT

Technical

7. PERIOD COVERED *(Inclusive Dates)*

8. PERFORMING ORGANIZATION — NAME AND ADDRESS *(If NRC, provide Division, Office or Region, U.S. Nuclear Regulatory Commission, and mailing address; if contractor, provide name and mailing address.)*

Idaho National Engineering Laboratory
EG&G Idaho, Inc.
P.O. Box 1625
Idaho Falls, ID 83415

9. SPONSORING ORGANIZATION — NAME AND ADDRESS *(If NRC, type "Same as above"; if contractor, provide NRC Division, Office or Region, U.S. Nuclear Regulatory Commission, and mailing address.)*

Division of Engineering
Office of Nuclear Regulatory Research
U.S. Nuclear Regulatory Commission
Washington, D.C. 20555

10. SUPPLEMENTARY NOTES

11. ABSTRACT *(200 words or less)*

Concrete barriers will be used as intimate parts of systems for isolation of low-level
radioactive wastes subsequent to disposal. This work reviews mathematical models for
estimating degradation rate of concrete in typical service environments. The models
considered cover sulfate attack, reinforcement corrosion, calcium hydroxide leaching,
carbonation, freeze/thaw, and cracking. Additionally, fluid flow, mass transport, and
geochemical properties of concrete are briefly reviewed. Example calculations included
illustrate the types of predictions expected of the models.

12. KEY WORDS/DESCRIPTORS *(List words or phrases that will assist researchers in locating the report.)*

Concrete barriers
Low-level radioactive waste
Mathematical models
Degradation rate of concrete

13. AVAILABILITY STATEMENT

Unlimited

14. SECURITY CLASSIFICATION

(This Page)

Unclassified

(This Report)

Unclassified

15. NUMBER OF PAGES

16. PRICE